

DEVELOPMENT OF A COLUMN MODEL TO PREDICT SILICA
BREAKTHROUGH IN A MIXED BED ION EXCHANGER

By

SHARMA PAMARTHY

Bachelor of Technology

Osmania University

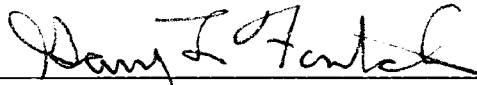
Hyderabad, AP, India

1992

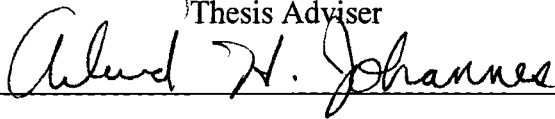
Submitted to the Faculty of the
Graduate College of the
Oklahoma State University
in partial fulfillment of
the requirements for
the Degree of
MASTER OF SCIENCE
May, 1996

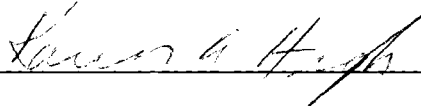
DEVELOPMENT OF A COLUMN MODEL TO PREDICT SILICA
BREAKTHROUGH IN A MIXED BED ION EXCHANGER

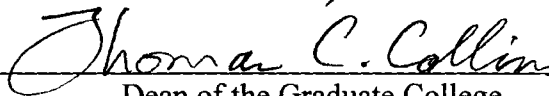
Thesis Approved:



Thesis Adviser







Dean of the Graduate College

TABLE OF CONTENTS

Chapter	Page
I. INTRODUCTION.....	1
II. LITERATURE REVIEW.....	3
Basic Principles of Ion Exchange.....	3
Ion Exchange Equilibria and Selectivity.....	4
Silica Chemistry.....	5
Silica Solubility.....	8
Ion Exchange Kinetics.....	9
Particle Diffusion Control.....	10
Film Diffusion Controls.....	11
III. MODEL DEVELOPMENT.....	13
Basis and Assumptions.....	13
Ion Flux Expression.....	15
Particle Rates.....	16
Material Balances.....	17
IV. RESULTS AND DISCUSSION.....	19
V. CONCLUSIONS.....	54
BIBLIOGRAPHY.....	56
APPENDIX A SILICA EQUILIBRIUM	
APPENDIX B MODEL PARAMETER VALUES	
APPENDIX C COMPUTER CODE FOR SILICA BREAKTHROUGH	

PREFACE

A computer model was developed to predict silica breakthrough in an ion exchange column. Column material balance equations are derived using the assumptions of film diffusion control and bulk phase neutralization. The variations in outlet concentrations due to various model parameters were studied. Most of the literature on ion exchange modeling addressing the removal of silica is qualitative in nature. This study extends this qualitative background and makes a first attempt at quantitative silica ion exchange issues. The silica particulates are accounted for in the model.

I wish to express my sincere gratitude to my advisor, Dr. Gary L. Foutch, for the continuous support and needful assistance throughout the course of this work. I would also like to thank Dr. Karen High and Dr. A. H. Johannes for serving on the advisory committee and for their technical help.

I would like to express special thanks to my parents, my sister and my younger brother for their moral support and continuous encouragement throughout my stay in the U.S.A. I wish to express my appreciation to Vikram Choudiah, Doctoral student at Oklahoma State University, for his technical assistance. I am also thankful to all my friends in the U.S.A and in India.

TABLE OF CONTENTS

Chapter	Page
I. INTRODUCTION	1
II. LITERATURE REVIEW	3
Basic Principles of Ion Exchange	3
Ion Exchange Equilibria and Selectivity.....	4
Silica Chemistry.....	5
Silica Solubility.....	8
Ion Exchange Kinetics	9
Particle Diffusion Control.....	10
Film Diffusion Controls.....	11
III. MODEL DEVELOPMENT	13
Basis and Assumptions	13
Ion Flux Expression	15
Particle Rates	16
Material Balances.....	17
IV. RESULTS AND DISCUSSION.....	19
V. CONCLUSIONS.....	54
BIBLIOGRAPHY.....	56
APPENDIX A SILICA EQUILIBRIUM	
APPENDIX B MODEL PARAMETER VALUES	
APPENDIX C COMPUTER CODE FOR SILICA BREAKTHROUGH	

LIST OF TABLES

Table	Page
I. Model Assumptions.....	19
II. Base Case Table	23

LIST OF FIGURES

Figure	Page
1. Effect of resin ratios on silica effluent concentrations.....	20
2. Effect of flow rate on silica breakthrough	22
3. Effect of temperature on silica effluent concentrations	25
4. Effect of particle size on silica breakthrough.....	26
5. Effect of the resin loadings on silica effluent concentrations	27
6. Effect of distance increment on silica breakthrough.....	29
7. Effect of time increment on silica effluent concentrations	30
8. Effect of Freundlich Coefficient on silica breakthrough	31
9. Effect of Freundlich index on silica effluent concentrations	33
10. Effect of Freundlich Adsorption Coefficient on particulate silica breakthrough.....	34
11. Effect of Freundlich Adsorption Coefficient on ionic silica breakthrough	35
12. Effect of Freundlich Adsorption Index on ionic silica effluent concentrations	36
13. Effect of Freundlich Adsorption Coefficient on colloidal silica breakthrough	37
14. Effect of Freundlich Adsorption Index on colloidal silica breakthrough	38
15. Effect of diffusivity on silica breakthrough	39
16. Effect of rate constant for polymerization on silica breakthrough.....	43
17. Effect of rate constant for hydrolysis on silica effluent concentrations.....	44
18. Effect of selectivity coefficient of silica on silica breakthrough.....	45
19. Effect of amorphous silica on particulate silica effluent concentrations	48
20. Effect of amorphous silica on colloidal silica breakthrough.....	49

21. Effect of amorphous silica on particulate silica effluent concentrations	50
22. Effect of Equilibrium Constant on particulate silica breakthrough	51
23. Breakthrough of all the participating ions.....	52
24. Effect of inlet concentration of ionic silica on silica breakthrough	53

NOMENCLATURE

a_s = interfacial surface area (L^2/L^3)

C_i = concentration of species I (meq/L^3)

C_i^* = concentration of resin in the resin (meq/L^3)

C_i^0 = concentration of resin in the bulk (meq/L^3)

d_p = particle diameter (L)

D_i = diffusivity of species i (L^2/T)

D_e = effective diffusivity for species i (L^2/T)

F = Faraday's constant (C/mole)

FAR = anionic resin volume fraction

FCR = cationic resin volume fraction

K_i = mass transfer coefficient (non-ionic) (L/T)

K_i' = mass transfer coefficient (ionic) (L/T)

K_A^B = resin selectivity for B compared to A

K_w = dissociation constant of water (mol/L^3)

Q = capacity of the resin (meq/L^3)

R = universal gas constant

R_i = ratio of mass transfer coefficients

T = temperature

t = time(T)

u = superficial velocity(L/T)

x_i = bulk phase concentration of species I

y_i = fraction of species I on the resin

Z_i = charge on species I

δ = film thickness (L)

ε = void fraction

ϕ = electric potential (ML^2/TC)

μ = viscosity of the bulk liquid (M/LT)

τ = dimensionless combined time-distance variable

ξ = dimensionless distance variable

Superscripts

o = bulk phase value

* = interfacial value

Subscripts

A = species A

B = species B

c = chloride ion

h = hydrogen ion

i = species i

j = species j

n = sodium ion

o = hydroxide ion

p = silica ion

x = potassium ion

w = water

Chapter I

Introduction

Deionization is a separation science. It differs from other separation processes such as distillation or leaching in that the matter being separated is charged ionic species. The process is one of stoichiometric reaction (Kunin, 1950). Electroneutrality of the system is maintained constant, implying that ionic species are exchanged on an equivalent basis. Ions are exchanged with ionic groups attached to the cationic and anionic exchangers. These exchangers are basically resins with fixed groups attached, such as sulfonic groups, etc. The charge on the resins determines whether they can be classified as cationic or anionic. The fixed charged groups have mobile ionic species bound weakly to them by Van der Waals forces to maintain electroneutrality with the resin. These mobile ions are exchanged freely with ions in solution having a like charge. The basic skeleton of an organic exchanger (anionic or cationic resin) is polystyrene with highly cross-linked divinyl benzene. Cross-linking increases the resin structure rigidity and affects the exchange kinetics.

Ion exchange can occur with cationic and anionic resin separately or intimately mixed together as a 'Mixed Bed.' In separate beds one ion type is removed followed by the other type. In a mixed bed, exchange occurs simultaneously. The effluent produced

by a mixed bed has less dissolved gases, ionic species, microbial impurities and particulates, including silica.

Cationic resin in the hydrogen form and anionic resin in the hydroxyl form exchange hydrogen and hydroxyl ions with the respective cations and anions of the feed. The hydrogen and hydroxyl ions equilibrate to form water. This, in turn, increases the driving force for exchange.

Ion exchange has many applications, primarily in the power, semi-conductor and pharmaceutical industries. These industries have very stringent water quality standards. Mixed-beds produce water which meets these requirements and is commonly referred to as "Ultra-Pure Water." Ultrapure water has ionic impurities less than $1\mu\text{g}/\text{Kg}$ (ppb), with correspondingly lower levels of particulates and microbial contaminants. The current impurity limit in many industries is in the range of ng/Kg (ppt). This demand is being met by employing membrane separation processes, such as electrodialysis and reverse osmosis, in combination with ion exchange. Some of these methods pretreat feed water to the ion exchangers, or polish the ultrapure water produced by ion exchange (Sadler, 1993).

The importance of particulate removal has increased tremendously in recent years. Silica and iron particulates must be removed from industrial waters to achieve ultra high purity. Silica is found to deposit on turbine blades and thereby reduce power plant efficiency (Iler, 1955). Particulates also adsorb onto microchips during machining of silicon wafers. This study addresses silica removal in its different forms from water. Soluble silica can be removed by ion exchange, but colloidal silica can be removed only by adsorption mechanisms.

Chapter II

Literature Review

This chapter is divided into two sections; the basic principles of ion exchange and the kinetic theories employed, and the chemistry of silica, its colloidal nature and the methods for its removal from water other than ion exchange. The kinetic discussion is similar to that of Haub (1984) and Zecchini (1990). The terminology used in this thesis is from Kunin (1950) and Helfferich (1962). This section follows the work done by Iler (1970), Hausen (19), and Owens (1985) in content and style. Silica removal by ion exchange is the main objective of this thesis.

Basic Principles of Ion Exchange

The resins used in ion exchange are prepared by copolymerization of a monomer, say styrene, with divinyl benzene (commonly referred to as DVB). Copolymerization causes DVB to cross-link with styrene. Cross-linking increases the rigidity of the resin. This is important because the resin should be resistant to “swelling,” “osmotic shock,” and other problems encountered in ion exchange. One significant resin classification is based on DVB mole percent. Desirable resin characteristics are listed below. They should:

- be negligibly soluble in solution (aqueous or non-aqueous),
- maintain structural rigidity and chemical stability,
- have consistent porosity and particle size, and

- be able to withstand fouling and corrosion.

The fixed charged groups determine the ion exchange behavior of the resins. Resin selectivity depends on the nature of these groups (Zuyi, 1993). Acidic or basic (charged) groups are fixed in the resin hydrocarbon matrix by heating in acids or bases for prolonged times. For instance, sulphonic groups are introduced by heating resin in sulfuric acid. These groups attract exchangeable ions of opposite charge. These “counterions” are exchanged for ions of like charge on an equivalent basis. The exchange of counterions ensures that electroneutrality is maintained within the exchanger and the bulk liquid. The number of sites available for exchange determines the resin “capacity,” expressed as meq/ml. The exchange equilibrium depends on resin selectivity.

Ion Exchange Equilibria and Selectivity

When an ion exchanger contacts an electrolyte solution, exchange will continue until equilibrium between the two phases is attained (Samuelson, 1963). Equilibrium depends on the properties and the quantities of the components in the system. Both the resin and liquid phase will have all components, but in different concentrations.

The exchange of two monovalent ions is represented by:



A and B refer to the counterions whereas A_r and B_r refer to the mobile ions attached to the resin. The forward reaction will not be favorable if the concentration of component B is large in the bulk liquid phase. For a simple exchange, the selectivity coefficient, K , is defined by the law of mass action as:

$$K_A^B = \frac{[A_r][B]}{[A][B_r]} \quad (\text{II-2})$$

where the brackets refer to the concentration in the bulk and the resin phases.

If the exchanging species have different charges, then the corresponding relation is:

$$K_B^A = \frac{[A_r]^a [B]^b}{[A]^a [B_r]^b} \quad (\text{II-3})$$

where a and b are the absolute values of exchanging ion valence. The selectivity coefficient has no units compared to the quantities used to calculate it (meq/ml., etc.) for univalent exchange.

The selectivity coefficient describes resin behavior. For $K_B^A > 1$, the resin has a strong affinity for A compared to B. If $K_B^A < 1$, the resin prefers B to A. If $K_B^A = 1.0$, the resin has no preference. Resins prefer counterions with higher valance, smaller equivalent volume, greater polarity and stronger association with the fixed charged groups in the matrix (Helfferich, 1962).

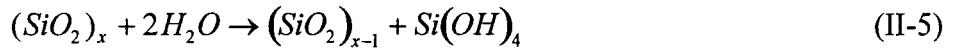
Silica Chemistry

Although silica is one of the most abundantly available materials in the earth's crust, not much is known about its chemistry. Recently its importance has been recognized and efforts are being directed at understanding its chemical nature. The solubility of silica in water is not yet completely understood since its dissolution in water is not simple. It involves a hydrolysis reaction:



where $\text{Si}(\text{OH})_4$ is known as silicic acid. Iler (1970) discusses silica in solution, similar to that of sugar in water, where some molecules exist in a crystalline state. Low condensation polymers such as $[[(\text{OH})_2\text{SiO}]_4]_n$ appear to be water miscible fluids, soluble silica or $\text{Si}(\text{OH})_4$, and would probably be a clear liquid in an anhydrous condition.

The dissolution and deposition of silica in water involves hydration and dehydration reactions which are evidently catalyzed by the hydroxyl ions.



where the forward reaction is hydration and the reverse is dehydration. The different silica forms participating in Reaction II-5 require explanation.

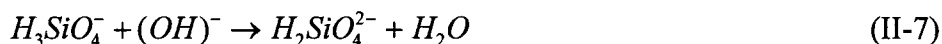
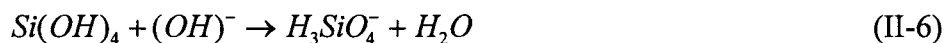
Amorphous silica: This form is most commonly seen. It exists as clays, massive dense amorphous glass, powders, gels, colloids, etc. Amorphous silica is soluble in water. The solubility is both temperature and pressure dependent (Iler, 1955). There are many correlations which describe the solubility of amorphous silica in water (Iler, 1970). Amorphous silica is more soluble in seawater at great depths due to the higher pressure. The solubility of “sands of seashore” is less compared to the amorphous silica that dissolves and enters into the water due to the weathering of minerals which leave behind amorphous silica residues which then dissolve as time goes by.

Amorphous silica can be broadly categorized as porous and non-porous. The solubility of non-porous amorphous silica is less than that of its porous counterpart. Porous amorphous silica has more sites for water to react, hydrate, and solubilize. Solubility is measured as SiO₂ (in parts per million) at a particular temperature. For non-porous amorphous silica, the equilibrium concentration at 25⁰C corresponds to 70 ppm as SiO₂. The most common forms of amorphous silica consist of porous aggregates which have Si-OH groups on their surfaces due to hydration. This form shows a higher solubility than the non-porous form. The equilibrium concentration of porous amorphous silica is in the range of 100-130 ppm as SiO₂. This is the reason for the higher solubility of gels and most powders.

Crystalline silica: The crystalline form is denser and more compact. The common forms are: quartz, flint, etc. Quartz is present almost universally as “sand.”

Quartz can exist in different phases depending on temperature; quartz, tridymite, cristobalite, keatite, coesite, and stishovite. The latter three are formed under high temperature and pressure. The solubility of crystalline silica is very low compared to other forms.

Soluble silica: The weathering of minerals causes silica to dissolve into water. Silica solubility is a function of temperature, pressure and pH (Iler, 1970). It is commonly referred to as monosilicic or orthosilicic acid, the chemical formula being $\text{Si}(\text{OH})_4$. Monosilicic acid has a tendency to polymerize at high concentrations with time, giving polysilicic acid, colloids, gels, sols, etc. These are amorphous forms. Monosilicic acid is a very weak acid and does not ionize in the presence of weak acids, but in an alkaline medium it does form ionic silica. Silicic acid is completely soluble at high pH. Monosilicic acid ionizes to give H_3SiO_4^- above pH 9. At pH 11, it ionizes further to yield $\text{H}_2\text{SiO}_4^{2-}$. The reactions are:



The equilibrium constants at 25°C for these reactions are known.

$$\frac{[\text{H}_3\text{SiO}_4^-]}{[\text{Si}(\text{OH})_4][\text{OH}^-]} = 1.5 \times 10^4 \quad (\text{II-8})$$

or

$$\frac{[\text{H}_3\text{SiO}_4^-][\text{H}^+]}{[\text{Si}(\text{OH})_4]} = 10^{-9.8} \quad (\text{II-9})$$

The equilibrium constant for Equation II-7 is:

$$\frac{[\text{H}_2\text{SiO}_4^{2-}]}{[\text{H}_3\text{SiO}_4^-][\text{OH}^-]} = 69.2 \quad (\text{II-10})$$

or

$$\frac{[H_2SiO_4^{2-}][H^+]}{[H_3SiO_4^-]} = 10^{-12.16} \quad (\text{II-11})$$

Silica is completely soluble above pH 11. Soluble silica is present in almost all water and found up to a few parts per million in animals. Silica is removed from water by biochemical activity and stored in these organisms. Silica reacts readily with metallic hydroxides like Al, Mg, etc. and is precipitated. This property allows precipitation as a pretreatment method for silica removal.

Silica Solubility:

Colloid science is needed to explain the most important phenomena of high-molecular organic compounds. Colloid science is the basis on which the properties of siliceous compounds can be explained (Hausen, 1960). To understand the colloidal nature of silica, it is important to know the solubility characteristics of silica. A detailed review of the solubilities of different phases of silica is provided by Iler (1970). An overview is presented here.

Solubility of crystalline silica: Originally it was thought that quartz showed no true solubility equilibrium when allowed to dissolve in water. Many investigations were made to determine this equilibrium. Van Lier (1965) determined a definite solubility equilibrium for pretreated, cleaned quartz surfaces. The Van Lier equation is:

$$\log C = 0.151 - \frac{1162}{T} \quad (\text{II-12})$$

where C is the molar concentration of soluble silica in parts per million and T is the absolute temperature (K). At ordinary temperatures, the solubility of quartz is around 10 ppm. Solubility of quartz under hydrothermal conditions was discussed by Kennedy (1950).

Solubility of amorphous silica: The equilibrium solubility for amorphous silica is not definite since studies vary (Iler, 1970). The reason for such results may be due to different particle sizes and impurities in the system. Different forms of amorphous silica have different equilibrium solubilities. This is because of the variations in the surface area per unit volume of the water available for the hydration reaction. Also, the attainment of equilibrium may take a very long time, since the hydration step is slow.

Solubility is a function of temperature, pressure and pH. For near neutral solutions solubility increases, and after a few days attains the equilibrium solubility asymptotically at that temperature and pressure. For higher pH, solubility increases rapidly with time. The solution might become supersaturated with silica which is relieved by the formation of colloidal silica. Thus, an equilibrium solubility of silica is attained. At lower pH, the solution increases linearly with an increase in pH of the solution. Silica solubility was found to be constant from pH 2 to 8 and then equilibrium solubility increased rapidly with pH. No particular number was agreed upon to account for the equilibrium solubility at standard temperature and pressure. The value is arbitrarily chosen owing to the different forms of amorphous silica available.

Ion Exchange Kinetics

Ion exchange kinetics can be described by three steps. They are:

- A film diffusion process, where mass transfer takes place from the bulk fluid to the resin surface.
- A particle diffusion process, where the mass transferred to the resin surface diffuses inside the resin phase.
- An exchange of the mass diffused inside the resin phase with that attached to the fixed groups.

In each of these steps, equivalent amounts of exchanging and exchanged species are moving counter to each other (Samuelson, 1963). Equilibrium is usually achieved quickly in ion exchange, depending on the degree of resin cross-linking. For a rigidly packed resin, the time required for equilibrium is significantly higher than for a resin which has a lower cross-linking. Column performance depends on ion exchange kinetics. It is therefore important to guess the right combination of rate-limiting reactions for the specific situation under consideration. Most ion exchange processes are diffusion-limited (Zecchini, 1990). The diffusion step can be charge transfer from the bulk liquid to the liquid film surrounding the resin, diffusion within the particle, or a combination of both processes.

Particle Diffusion Control

An essential assumption is that electroneutrality be maintained within the ion exchanger. Therefore, the concentration of the fixed charged groups should equal the total counterion concentration.

Mathematically, this can be expressed as:

$$Z_A C_A^* + Z_B C_B^* = C^* \quad (\text{II-13})$$

where,

C^* = total concentration of fixed charged groups in the resin (meq/cm³)

Writing a similar expression for the counterion fluxes,

$$Z_A J_A^* + Z_B J_B^* = 0 \quad (\text{II-14})$$

where,

J_I^* = flux of species I (meq/sec·cm²)

Flux can be defined by either Fick's first law of diffusion or the Nernst-Planck equation. The Nernst-Planck equation has an additional term, electric potential due to the

different ionic mobilities, which affects the exchange rate. The flux is related to the concentration gradient by using a diffusion coefficient. The Nernst-Planck equation for species i is:

$$J_i = D_i \left(\nabla C_i + \frac{Z_i F C_i}{RT} \nabla \phi \right) \quad (\text{II-15})$$

where,

D_i = Diffusion coefficient of species i (cm^2/s)

F = Faraday's constant (coulombs/mole)

R = universal gas constant (ergs/mole.K)

ϕ = Electric potential (ergs/coulomb)

T = absolute temperature (K)

The first part of the equation is Fick's first law, the second part is the flux due to an external driving force. It should be understood that there is no external electric field applied to the exchanger, only an induced electric field is produced due to the differing ionic mobilities and at low concentrations, the dissociative nature of water. The above equation is used in conjunction with the static-film model (Zecchini, 1991).

Combining the Nernst-Planck equation with the flux expression and electroneutrality gives:

$$J_B = -D \text{ grad}(C_B^*) \quad (\text{II-16})$$

where, the effective diffusivity is defined as:

$$D^* = D_A^* D_B^* \frac{(Z_A^2 C_A + Z_B^2 C_B)}{(Z_A^2 C_A D_A^* + Z_B^2 C_B D_B^*)} \quad (\text{II-17})$$

Film Diffusion Controls

The assumptions of film diffusion are:

- a stagnant film of uniform thickness surrounds the resin bead,
- the curvature of the film is neglected, and
- a sharp boundary exists separating the bulk liquid and the liquid film.

The liquid film can be modeled by employing various concepts such as a hydraulic radius film model, boundary layer model and the Nernst static film model. The Nernst-Planck equation can describe the diffusion process in the liquid film. In order to apply the Nernst-Planck equation for ionic flux, we need to use the hydraulic radius film model for the liquid film.

In order to calculate the exchange rates, we need a mass transfer coefficient for packed beds. Correlations of Carberry (1960) and Kataoka (1987) are used to obtain the non-ionic mass transfer coefficients.

Carberry's equation is:

$$K_1 = 1.15 \left(\frac{\mu}{\varepsilon} \right) (Sc)^{-2/3} (Re)^{-1/2} \quad (\text{II-18})$$

where,

K_1 = non-ionic mass transfer coefficient (cm/s)

ε = bed void fraction

μ = superficial liquid velocity (cm/s)

Sc = Schmidt number

Re = Reynolds number

Kataoka's equation is:

$$K_1 = 1.85 \left(\frac{\mu}{\varepsilon} \right) \left(\frac{\varepsilon}{1 - \varepsilon} \right)^{1/3} (Sc)^{-2/3} (Re)^{-2/3} \quad (\text{II-19})$$

In the model, we used Kataoka's correlation for low Reynolds number region (less than 20) and Carberry's relation otherwise.

Chapter III

Model Development

Basis and Assumptions

Although extensive literature on the modeling of ion exchange columns is available, no universal model can be applied to any exchange column under consideration. It is easier to model an ion exchanger for specific problems with a great emphasis on all the details of the problems. However, accounting for all the details increases the model complexity. In order to solve this problem, we need to make assumptions which simplify the model. Since employing assumptions may lead to erroneous results in predictions, caution is recommended before using any assumptions that might affect the desired accuracy of the model. The following model development is different from previous models in that it is more rigorous in nature and requires greater calculational effort. There is a need to optimize the present model in order to reduce the calculational load. The model also lacks supporting data required to obtain reasonably accurate predictions. The model is a continuation of the modeling effort started by Haub and Foutch (1984) and continued by Zecchini and Foutch (1990). The present model gives insight into the behavior of soluble and colloidal silica in industrial waters at very low concentrations. The model developed by Zecchini (1990) has a limited number of assumptions to give as general a model as possible. The present model is also fairly general but can be employed only for Mixed Bed Ion Exchange (MBIE) columns. This

restriction was used because only MBIE columns produce water with minimal amounts of contaminants.

The chief assumption is that the model is applicable only for processes which are film diffusion controlled where the Nernst-Planck equation can be used. Particle diffusion in the resin is neglected in this development. The rate of neutralization is quite high compared to the rate of exchange. So, neutralization is considered to be instantaneous. Other assumptions included in the model development are: uniform bulk-liquid and resin-phase compositions for a given ion exchanger, bulk-phase neutralization, equilibrium at the particle-film interface, activity coefficients equal to unity, pseudo-steady state mass transfer, isothermal operation, plug flow, and negligible axial dispersion. If activity coefficients are not taken as unity then we may need to calculate them using the Debye-Huckel equation (Stumm and Morgan, 1981). The above assumptions do not appreciably affect the predictions for an MBIE column except for the assumption of negligible axial dispersion which may have a pronounced effect for low flow rates through the ion exchanger. The additional term in the column material balance equation accounting for axial dispersion is negligible for high flow rates. For a more general model, we may include axial dispersion to get more accurate estimates at lower flow rates.

The assumption that the resin-phase and bulk-liquid composition near a resin surface does not change may not be true. Concentration profiles are bound to develop both in the bulk liquid and in the liquid film adjacent to the resin. We cannot account for these complexities in the model. This assumption greatly simplifies the model and solutions.

Table I
Model Assumptions

-
- 1) Film diffusion limited
 - 2) Pseudo steady state process
 - 3) No coion flux across the particle surface
 - 4) A static film surrounds the film adhering to the resin surface
 - 5) All univalent exchange
 - 6) Neutralization reactions are instantaneous compared to the ion exchange steps
 - 7) Resin-film interface is maintained at equilibrium
 - 8) The flux can be expressed using Nernst-Planck equation
 - 9) Curvature of the film can be neglected
 - 10) No net coion flux within the film
 - 11) Uniform bulk liquid and resin phase compositions
 - 12) Activity coefficients equal to unity
 - 13) Plug flow
 - 14) Isothermal operation
 - 15) Negligible axial dispersion

Ion Flux Expressions

The Nernst-Planck equation for ion i can be written mathematically as:

$$J_i = D_i \left(\nabla C_i + \frac{Z_i F C_i}{RT} \nabla \phi \right) \quad (\text{III-1})$$

Equation III-1, when used in conjunction with the static film model, gives us a relationship for the anionic flux in terms of the diffusivities and the bulk phase concentrations of the anions. The detailed derivation is shown in Appendix A. The final equation for the anionic flux is:

$$J_c = 2 \frac{D_c D_o}{(D_c - D_o) \delta} (C_c^o + C_o^o - C_c^* - C_o^*) \quad (\text{III-2})$$

a similar expression can be derived for cationic flux and both may be combined to define the effective diffusivity for each species.

Particle Rates

The static film model can be used to define the particle rate as:

$$\frac{\partial \langle C_i \rangle}{\partial t} = K_1 a_s (C_i^o - C_i^*) \quad (\text{III-3})$$

where $\langle C_i \rangle$ is the resin phase concentration of species I, and K_i' is the mass transfer coefficient for the ion exchange process. An R_i factor relates this mass transfer coefficient to the non-ionic mass transfer coefficient determined by either Kataoka's (1987) or Carberry's correlation (1960). The factor can be determined from the effective diffusivity for each ion. It is related to the effective diffusivity by:

$$R_i = \left(\frac{D_e}{D_i}\right)^{2/3} = \frac{K_i'}{K_i} \quad (\text{III-4})$$

Let us represent the total resin capacity as Q and the total counterion as C_T .

Hence, we can define the resin and liquid phase fractions.

The resin phase fraction is defined as:

$$y_i = \frac{\langle C_i \rangle}{Q} \quad (\text{III-5})$$

Similarly, the liquid phase fractional concentration is:

$$x_i = \frac{C_i}{C_T} \quad (\text{III-6})$$

Equations III-3 to III-6 can be combined to give:

$$\frac{\partial y_i}{\partial t} = K_i R_i a_s C_T \frac{(x_i^o - x_i^*)}{Q} \quad (\text{III-7})$$

Material Balances

The column material balance determines the concentration profile of the ion exchange column and estimates the outlet concentration for each ionic species. The material balance equation is:

$$\left(\frac{u}{\varepsilon}\right) \frac{\partial C_n}{\partial z} + \frac{\partial C_n}{\partial t} + \frac{(1-\varepsilon)}{\varepsilon} \frac{\partial q_n}{\partial t} = D_L \frac{\partial^2 C_n}{\partial z^2} \quad (\text{III-8})$$

The Right Hand Side (R.H.S) of the above equation becomes zero when axial dispersion is neglected. For the model, therefore, R.H.S is equal to zero. The above equation is for one ion exchanger only. Kataoka (1987) has modified Equation III-8 to incorporate the volume fractions of both the cationic and anionic resins into the material balance equation. Certain dimensionless quantities are employed for this purpose. The details of this derivation are given in Appendix D.

Freundlich equations are used to estimate a rough value for the interfacial concentration of ionic silica. The formula employed is given below:

$$CPI = \left(\frac{1.0}{a1} \times YP\right) \times \left(\frac{1.0}{e1}\right) \quad (\text{III-9})$$

where, CPI is the interfacial concentration for ionic silica, YP is the resin loading for silica, e1 and a1 are the Freundlich index and Freundlich coefficient, respectively.

Freundlich adsorption isotherms are used to calculate the amounts of particulate silica, amorphous silica, colloidal silica adsorbed onto the anionic resin. Mathematically this can be expressed as:

$$SXADS = SXADS + Ax(SXSILxxB) \quad (\text{III-10})$$

$$PARADS = PARADS + Ax(PARSILxxB) \quad (\text{III-11})$$

$$COLADS = COLADS + Ax(COLSILxB) \quad (III-12)$$

where, SXADS, PARADS, COLADS are the adsorbed forms of amorphous, particulate and colloidal silica, respectively and SXSIL, PARSIL, COLSIL are the amorphous, particulate and colloidal forms of silica, respectively. A and B are the Freundlich coefficient and Freundlich index, respectively.

Chapter IV

RESULTS AND DISCUSSION

The model was developed to account for breakthrough of monovalent ionic silica, and estimate the amount of particulate silica removed by adsorption on anion exchange resin employing adsorption isotherms. Also, the present model can predict the colloidal silica formed in the ion exchange column and the amount of colloidal silica that can be removed by adsorption. The various model parameters considered during the development are listed in Appendix C.

The volume fraction of the anion exchange resin has a remarkable effect on the monovalent ionic silica breakthrough from the exchanger. For an anion exchange resin fraction of 0.6, the breakthrough for monovalent silica was found to occur at around 45 days, but, for an anion exchange resin fraction of 0.7, breakthrough occurred after 52 days. An earlier breakthrough was observed when the anionic resin fraction is equal to 0.5. The observed breakthrough was after 35 days. These observations were expected because the number of ion exchange sites available increased with an increase in the anion resin ratio and vice-versa. With an increase in the number of sites, the resin could exchange more ionic silica than in the previous case, causing a delay in ionic breakthrough. Similarly, with a decrease in the anionic resin ratio, the number of sites available for exchange of ionic silica have decreased proportionately, leading to an earlier breakthrough. The plots for these simulations are shown in Figure 1.

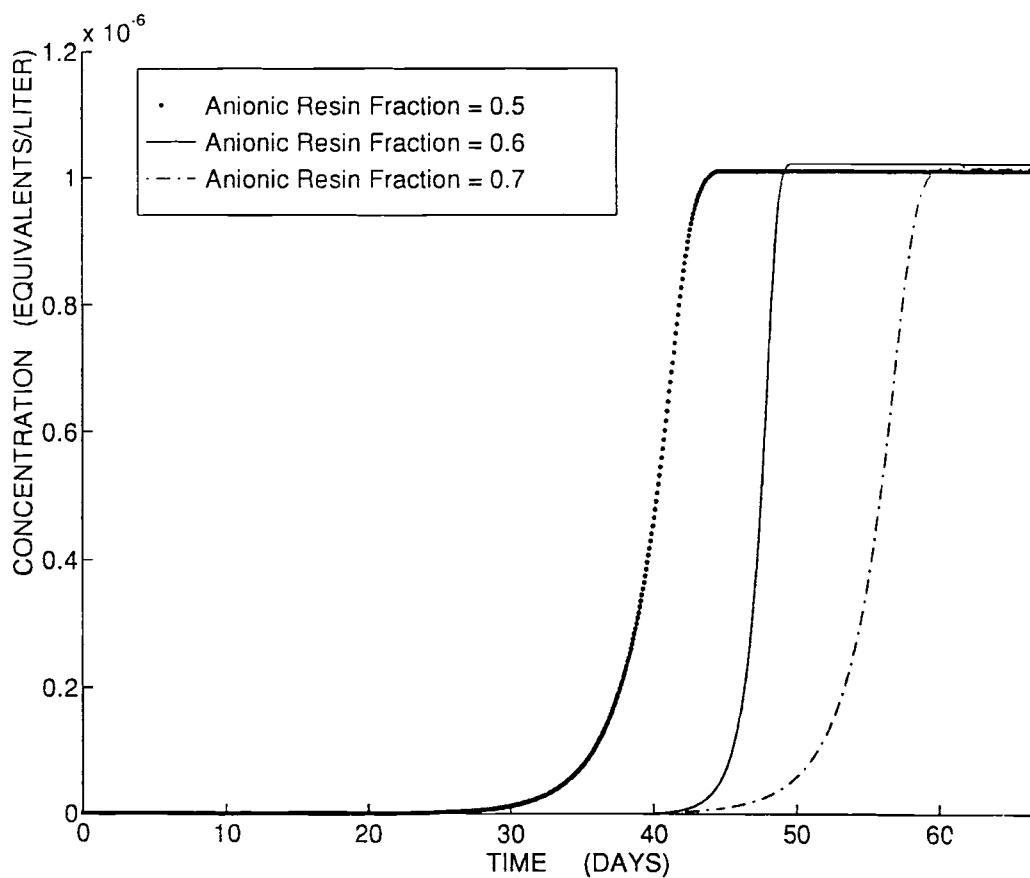


Figure 1. Effect of anionic resin fraction on silica effluent concentrations

The column dimensions that were considered in this study are:

column diameter: 100 cm

column height: 250 cm

flow rate of water: 1.25×10^5 ml/s

Anionic resin fraction: 0.6

The breakthrough time of monovalent anionic silica was found to increase with a decrease in the influent flow rate of the service water and decrease with an increase in the flow rate entering the ion exchange column. Three different cases with different influent flow rates are considered. With a flow rate of 1.25×10^5 ml/s, the breakthrough was found to occur after 45 days. But, with flow rates of 0.75×10^5 ml/s and 1.75×10^5 ml/s, the breakthrough of ionic silica is estimated to occur after 75 days and 32 days, respectively. Considering the latter case, this is also a reasonable estimate as the Reynolds number increases in direct proportion with the flow rate of the influent. This increase in Reynolds number causes a decrease in the mass transfer coefficient of the exchanger, as Reynolds number appears in the denominator of the formulas used in both Carberry's and Kataoka's mass transfer models. This decrease in the mass transfer coefficient causes less ionic silica to be taken up by the anionic resin. This causes an earlier breakthrough of ionic silica. Similar reasoning can also be applied to the former case where the flow rate was decreased (0.5×10^5 ml/s). In this case the Reynolds number is lower compared to the base case (1.25×10^5 ml/s). So, the mass transfer coefficient is correspondingly higher. With an increase in the mass transfer coefficient, the amount of ionic silica being taken up by the anionic resin increases correspondingly. So, a delayed breakthrough is expected. The results confirm this. The effect of flow rate on the breakthrough of ionic silica is shown in Figure 2.

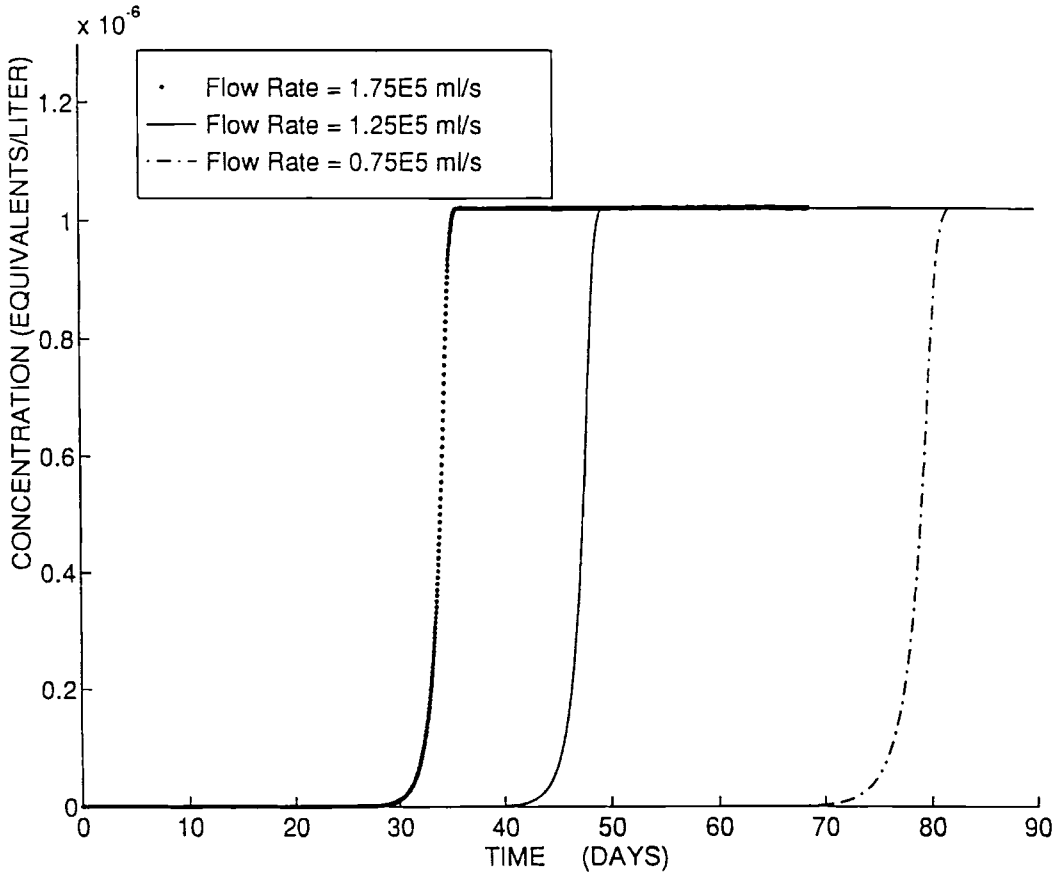


Figure 2. Effect of flow rate on silica breakthrough

**MODEL PARAMETER VALUES
FOR THE BASE CASE**

The various model parameters and their numerical values used for the base case are given below.

Initial fractions of sodium and potassium on the cationic resin	0.00001
Initial fractions of chloride on the anionic resin	0.0001
Initial fractions of silica on the anionic resin	0.00001
Particle diameter of the anionic resin (cm)	0.06
Particle diameter of the cationic resin (cm)	0.06
Void fraction of the bed	0.42
Volumetric Flow rate of the column influent (ml/sec)	1.25×10^5
Diameter of the column (cm)	2.5×10^2
Height of the column (cm)	1.0×10^2
Dimensionless time increment	0.002
Dimensionless distance increment	0.004
Cationic resin volume fraction	0.40
Density of the solution (g/cc)	1.0
Capacity of the Cationic resin	2.0
Capacity of the Anionic resin	1.2
Anionic resin volume fraction	0.6
Influent pH	7.0
Temperature of the influent (C)	25
Initial Concentrations of sodium and potassium entering the column	1.0×10^{-6}
Initial Concentrations of chloride and silica entering the column	1.0×10^{-6}
Equilibrium constant for the hydrolysis of amorphous silica	1.995×10^{-6}
Equilibrium constant for the ionization of soluble silica	1.85×10^4
Freundlich coefficient for calculating interfacial concentration of monovalent ionic silica	2.0
Freundlich index for calculating interfacial concentration of monovalent ionic silica	0.2
Freundlich adsorption coefficient	2.0
Freundlich adsorption index	4.0
Ionic conductivity of monovalent silica	50
Initial concentration of amorphous silica entering into the column	15 PPM
Selectivity coefficient for chloride-hydroxide exchange	16.0
Selectivity coefficient for silica-hydroxide exchange	2.5
Rate constant for polymerization of colloidal silica (1/day)	0.05
Rate constant for hydrolysis of colloidal silica (1/day)	0.20

Changes in temperature of the influent effects many physical properties of the fluid flowing through the bed. The various parameters effected by temperature: density, and viscosity of service water, diffusivity of the ions, dissociation constant for water, equilibrium constants, selectivity coefficients, rate constants for polymerization and hydrolysis of polymeric silica. Silica tends to polymerize on the anionic exchanger with time. But, when the temperature of the service water is high, silica polymerized on to the anionic exchanger is desorbed back into the water as soluble silica. Thus, the amount of soluble silica increases with an increase in the service water temperature. Silica in the lower band of the ion exchanger enters into the water and is seen as 'silica leakage' in the effluent water stream. Therefore, it takes less time for silica to break through as the temperature is increased.

Three cases are considered to explicitly show the temperature effect on 5 breakthrough of ionic silica. The base case is at 25⁰ C. The ionic silica breakthrough is 18 days. For 30⁰ C and 50⁰ C, the breakthrough times were found to be 13 and 11 days, respectively. The predictions from the simulations are in accordance with the above discussion. The plots for these simulations are shown in Figure 3. The anionic resin fraction in this case was 0.4.

One of the most important properties of an ion exchanger is the size of the resin bead. The particle diameter of the anion exchanger was found to effect ionic silica breakthrough. Three different cases are considered here. The base case is with an anion particle diameter of 0.06 cm. Particle diameters of 0.08 cm and 0.10 cm are used for the second and the third cases, respectively. The simulations for these three cases show that the breakthrough for ionic silica increased with an increase in the particle diameter. The breakthrough curves for the three cases are 45, 46 and 47 days. An increase in the resin diameter increases the particle Reynolds number which decreases the particle mass transfer coefficient. A decrease in the particle mass transfer coefficient decreases the rate

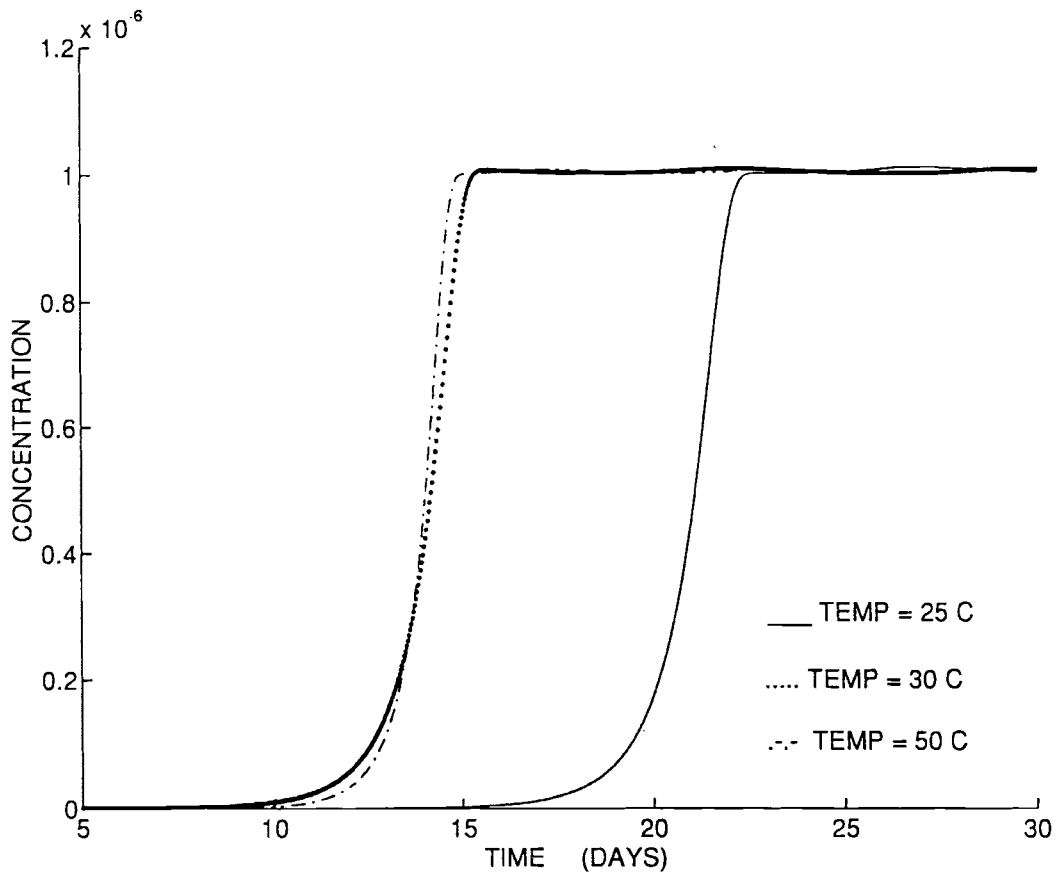


Figure3. Effect of temperature on ionic silica effluent concentrations

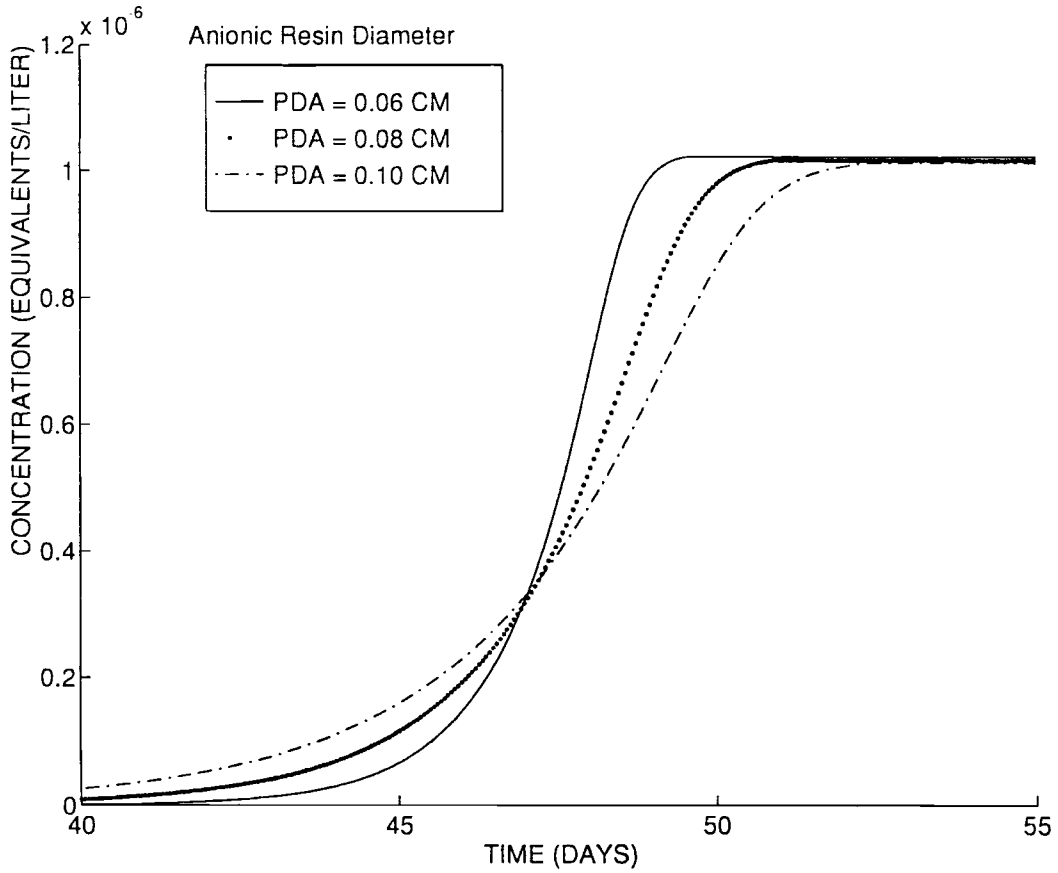


Figure 4. Effect of particle size on ionic silica breakthrough

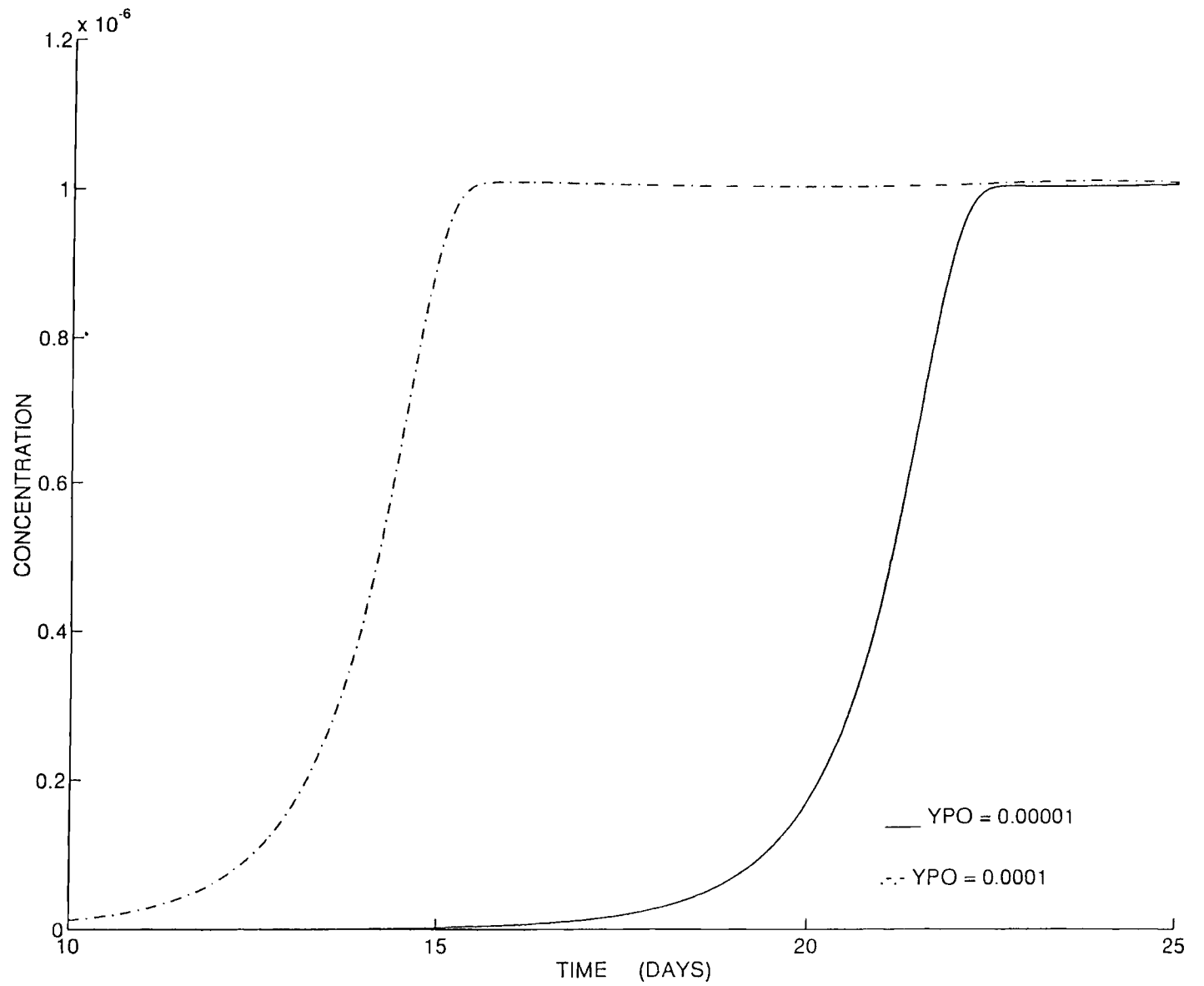


Figure 5. Effect of the resin loadings on silica effluent concentrations

exchange of ionic silica onto the resin. This produces a lag in breakthrough curves of smaller particle diameters. Figure 4 shows the variation of the breakthrough curves with the particle size.

The resin loading effects breakthrough, as observed from the breakthrough curves for two column simulations with different anionic resin loading. The first case is with a silica loading of 10^{-5} . The second case is with a silica loading of 10^{-3} . The rest of the parameters were the same for both cases. The anionic resin fraction in both the cases was 0.4. Column simulations show in the former case, that the onset of breakthrough occurred after 20 days. In the latter case, breakthrough occurred after 12 days. The prediction is reasonable because with an increase in the initial resin loading of the anionic resin, the resin can no longer exchange the same amount of ionic silica as in the earlier case with lesser initial resin loading. That is, the resin's capacity to exchange ionic silica decreases with an increase in the resin loading. The column simulations are, therefore, reasonable. The simulations are shown in Figure 5.

Figures 6 and 7 show us the variation of breakthroughs with variations in the distance and time increments, respectively. These two parameters were found to effect the stability of the system. Variation in the time increments was found to have a more pronounced effect on the output concentrations of ionic silica than the variation in the distance increments.

The effect of the Freundlich coefficient used in the calculation of the anionic interfacial concentrations for ionic silica is shown in Figure 8. Three different cases are considered here. The base case uses a Freundlich coefficient (a_1) of 4.0. The other two cases are for 6.0 and 8.0. The breakthrough curves for the three cases are: 45 days, 68 days, and 105 days. It is obvious that the breakthrough times for ionic silica are directly proportional to the Freundlich coefficient. The reason for this type of behavior is due to the presence of the Freundlich coefficient in the denominator of the formula used to estimate the interfacial concentration of ionic silica. With an increase in the value of the

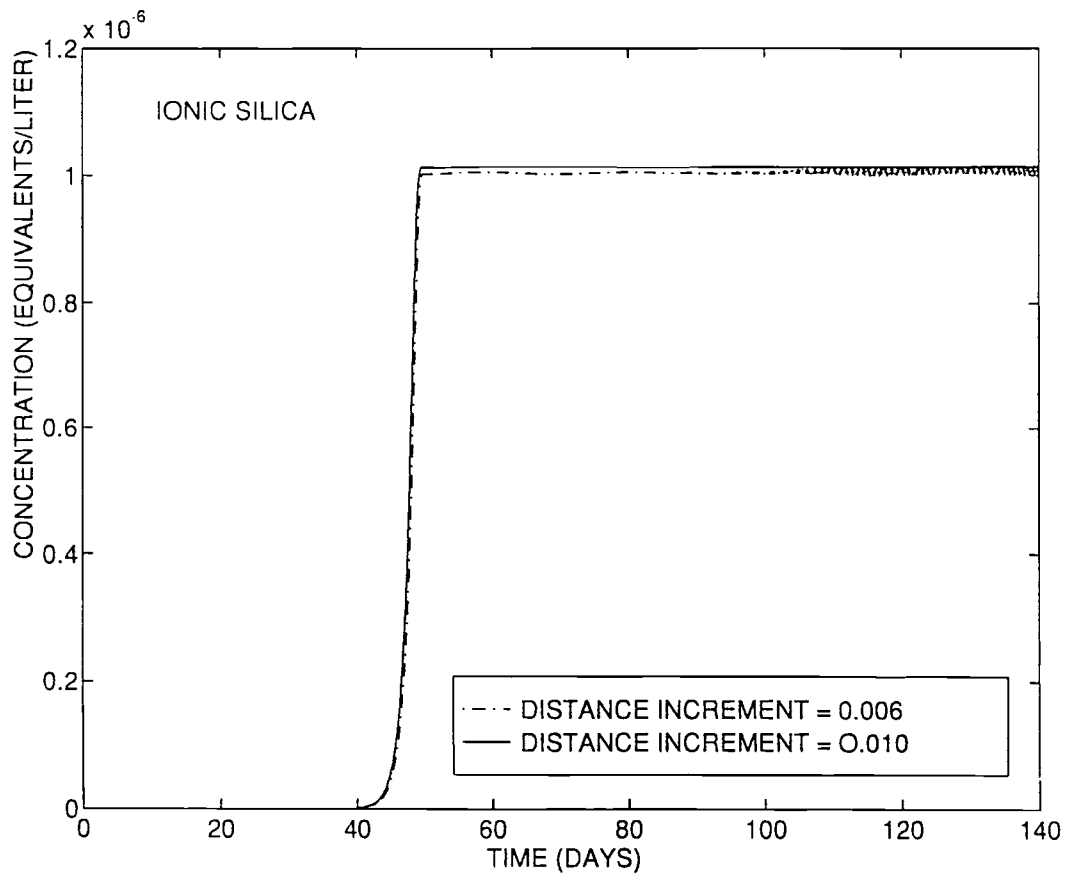


Figure 6. Effect of distance increment on silica breakthrough

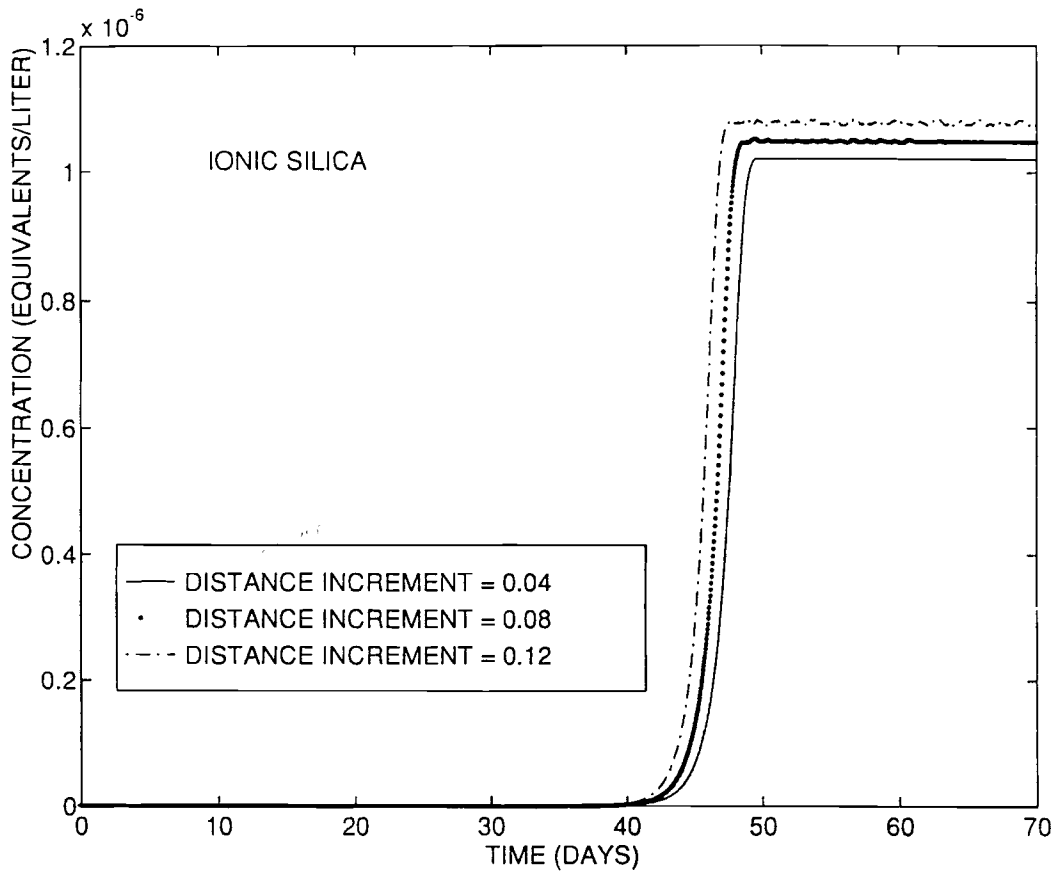


Figure 7. Effect of time increment on silica effluent concentrations

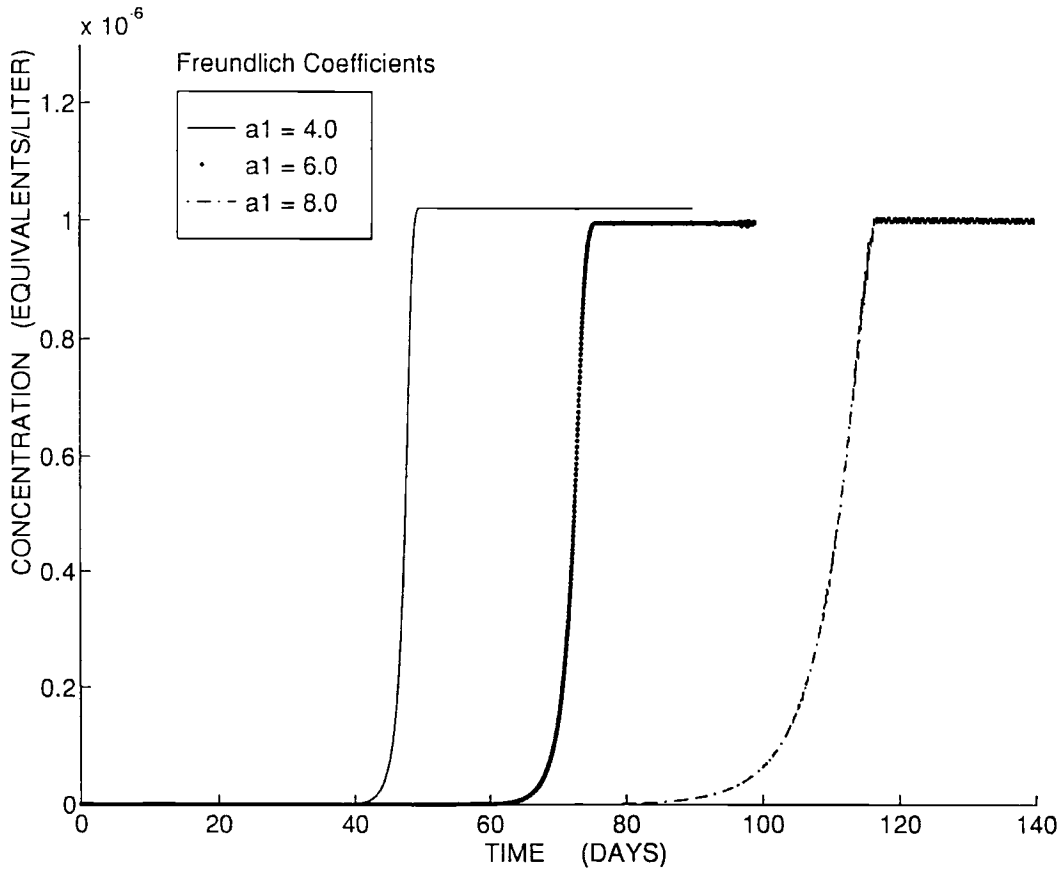


Figure 8. Effect of Freundlich Coefficient on silica breakthrough

Freundlich coefficient the interfacial concentration decreases. This decrease in the interfacial concentration causes the rate of ion exchange to increase. An increase in the rate of ion exchange causes more ionic silica to be exchanged by the anionic resin and this causes a delayed breakthrough for ionic silica. We selected a value of 4.0, as we know that ionic silica is the first to show up in the column effluent as ‘silica leakage’. This is because, as was mentioned earlier, silica forms the weakest known acid, silicic acid, which is not exchanged with great affinity onto the anionic resin when compared to other acids such as hydrochloric acid (from chloride ions) and sulfuric acid (from sulfate ions).

Similarly, we note the effect of the Freundlich index on the breakthrough of ionic silica. Two cases are presented here. The value of the Freundlich index used for the base case is “ e_1 ” = 0.2. For values higher than 0.2, a lot of instability was observed in the plots. For the other case, the value of “ e_1 ” was set equal to 0.15. The rest of the parameters are the same for both cases. For “ e_1 ” = 0.15, we observe that the breakthrough was delayed to 85 days, compared to the base case of 45 days. This is evident from the Freundlich formula, shown earlier, used to calculate the interfacial concentration of ionic silica. The same reasoning as in the case of Freundlich coefficient can be applied here. As “ e_1 ” appears in the denominator of the formula used to calculate the interfacial concentration, the interfacial concentration would decrease with an increase in the value of “ e_1 ”. This decrease in the interfacial concentration leads to an increase in the rate of ion exchange, and ultimately to a delay in breakthrough. The simulations can be seen in Figure 9.

Figures 10, 11, and 13 show the effect of Freundlich Adsorption Coefficient on particulate, ionic, and colloidal forms of silica, respectively. Similarly, Figures 12 and 14 describe the variation of breakthrough curves for ionic, and colloidal forms of silica with variation in the Freundlich Adsorption Index. The effects were not as pronounced as in the earlier cases of Freundlich Coefficient, and Freundlich Index (Figures 8 and 9). This is because in the former case, only the bulk concentrations of different forms of silica

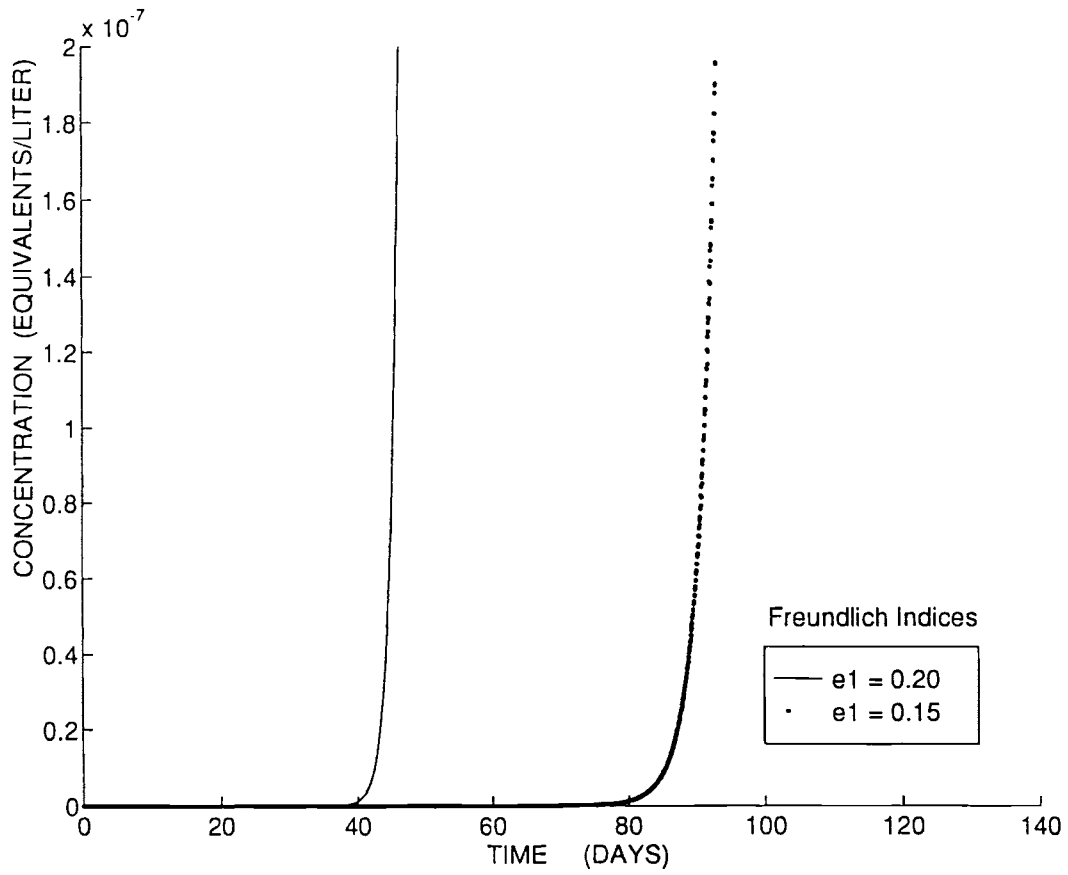


Figure 9. Effect of Freundlich index on silica effluent concentrations

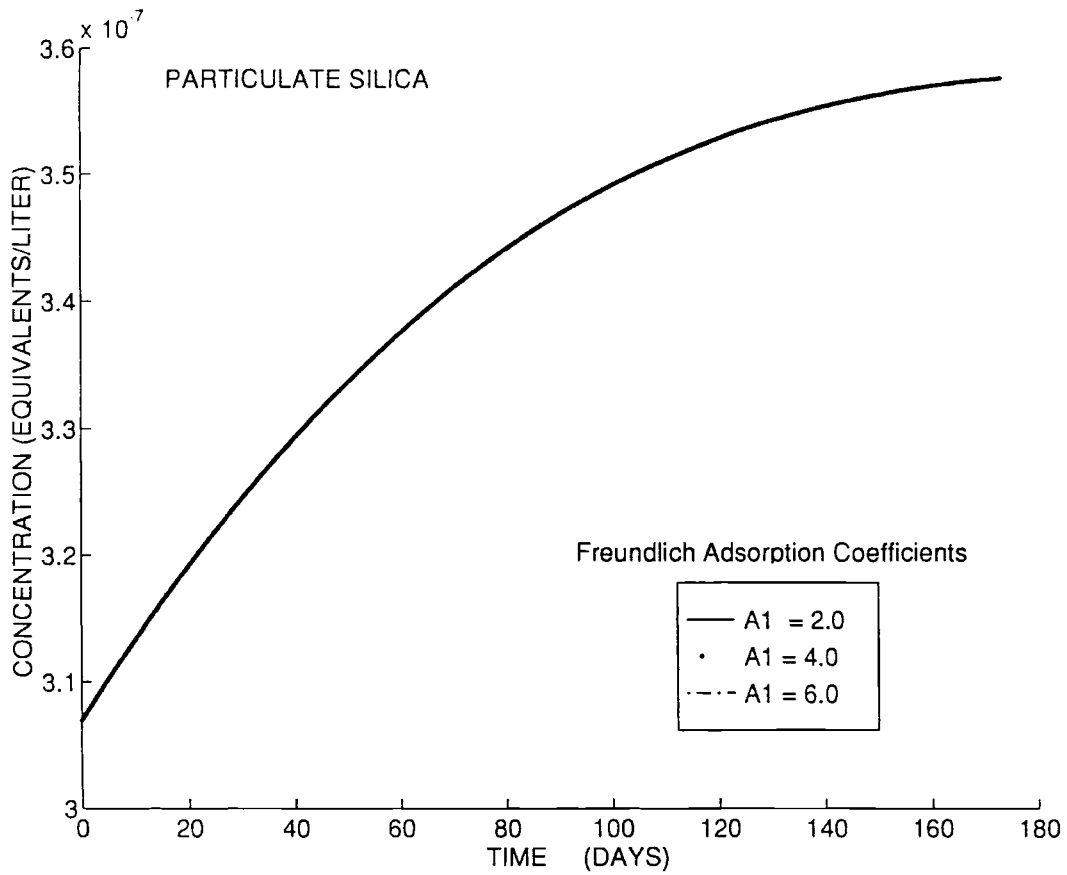


Figure 10. Effect of Freundlich Adsorption Coefficient on particulate silica breakthrough

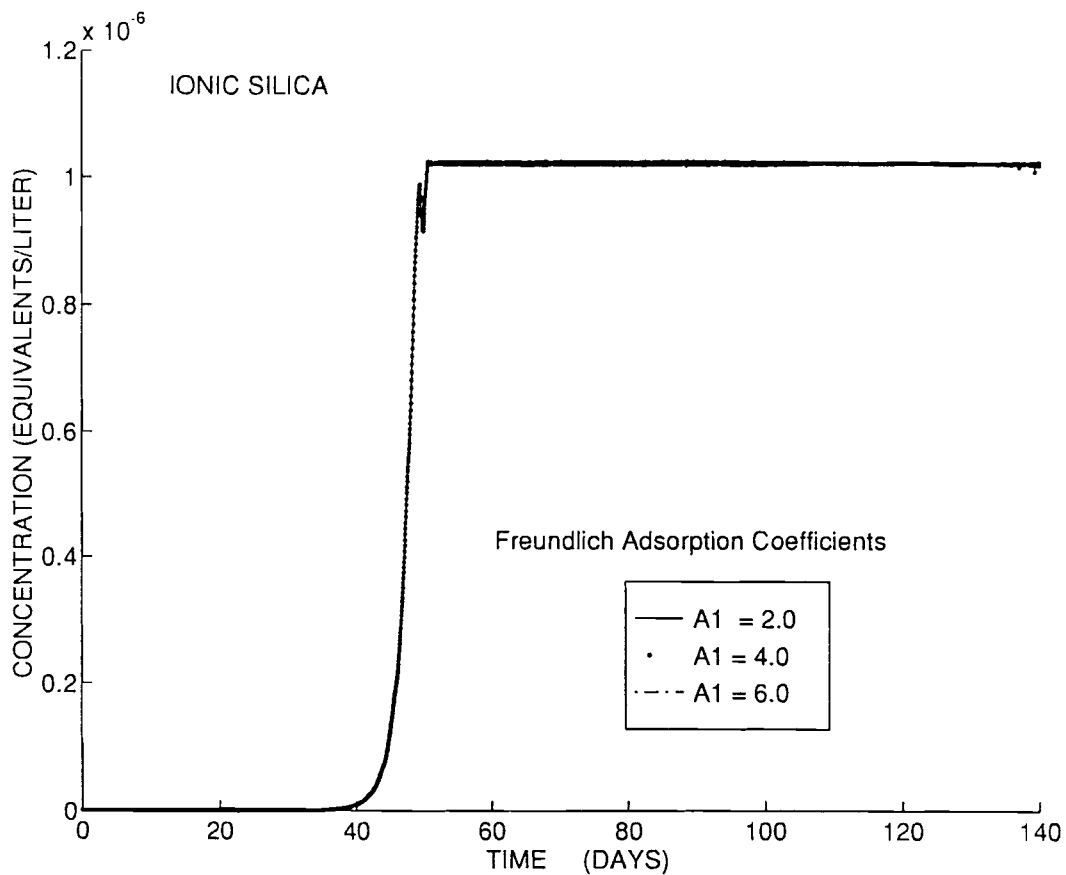


Figure 11. Effect of Freundlich Adsorption Coefficient on ionic silica breakthrough

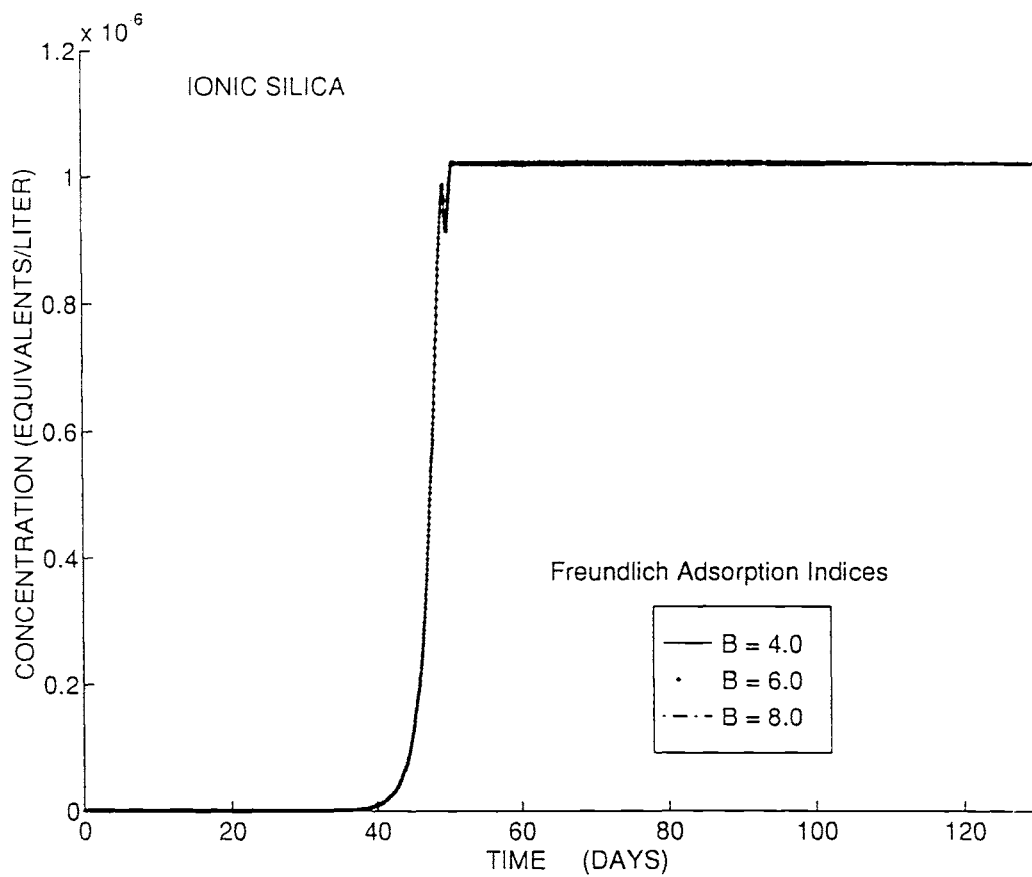


Figure 12. Effect of Freundlich Adsorption Index on ionic silica effluent concentrations

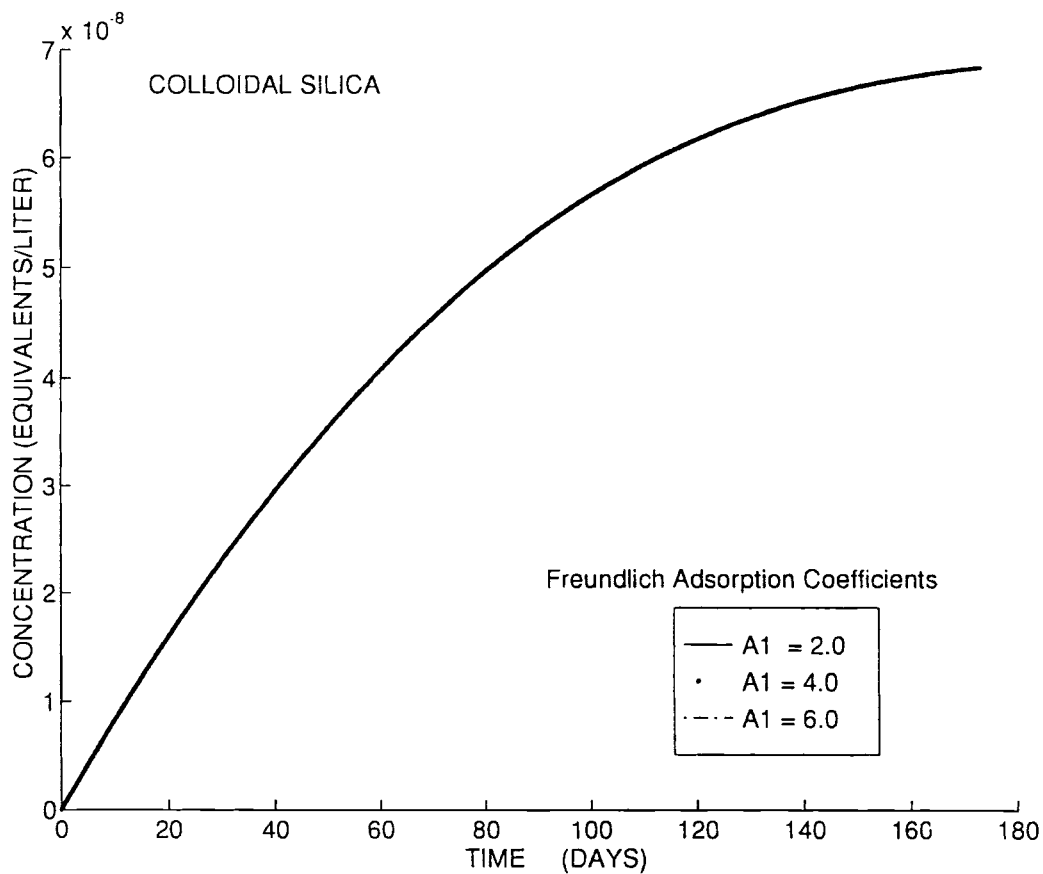


Figure 13. Effect of Freundlich Adsorption Coefficient on colloidal silica breakthrough

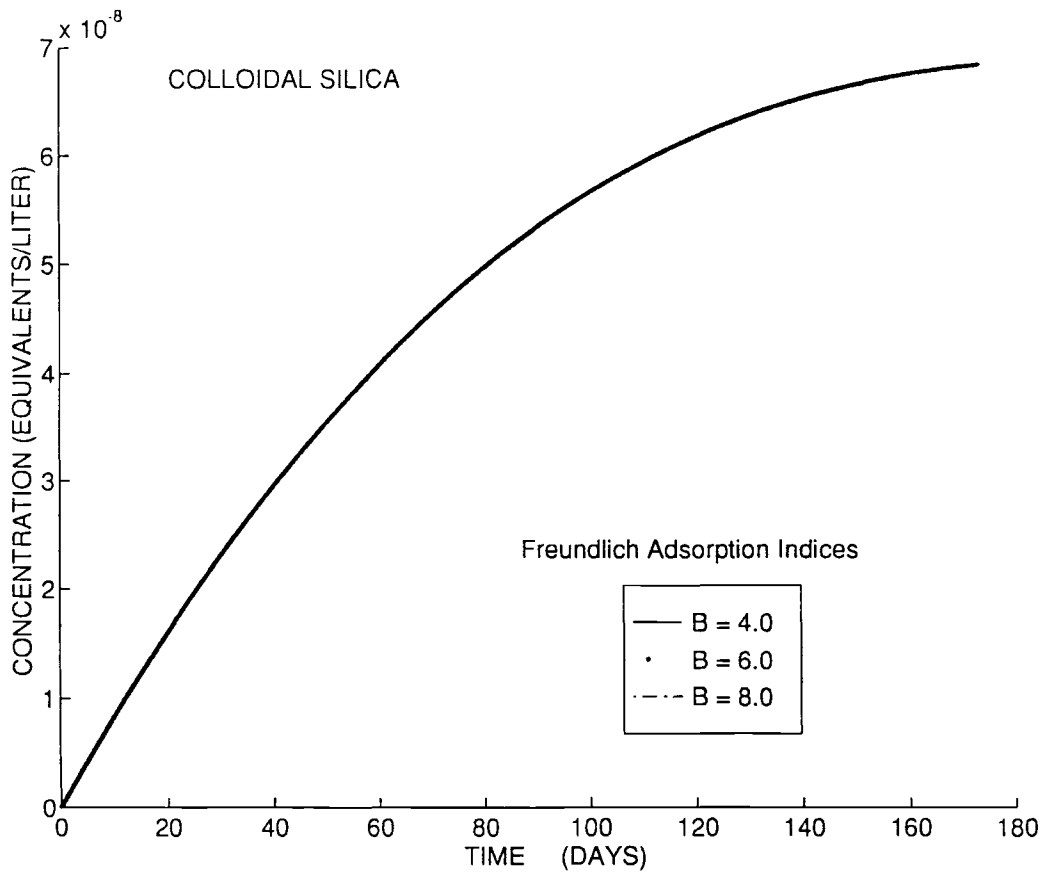


Figure 14. Effect of Freundlich Adsorption Index on colloidal silica breakthrough

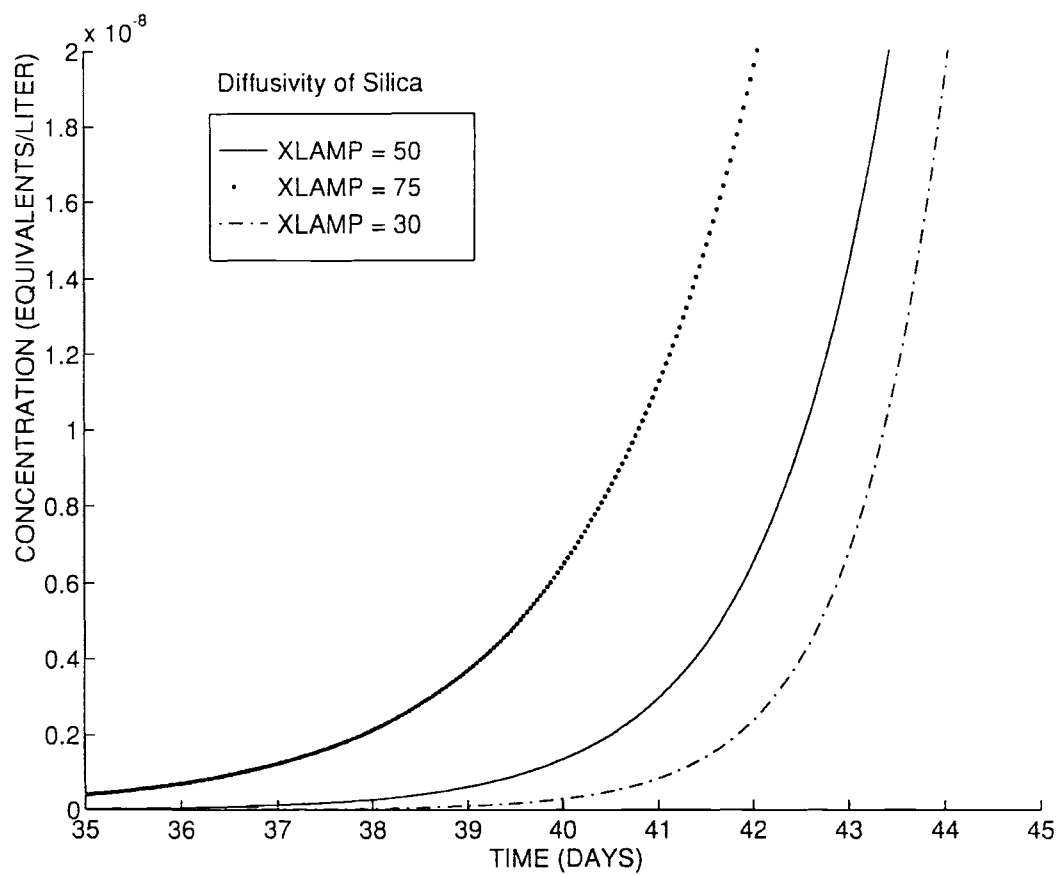


Figure 15. Effect of diffusivity on silica breakthrough

were found to change with changes in the Adsorption Coefficient, and Adsorption Index, whereas in the latter case the interfacial concentrations were found to vary. The rate of exchange is more strongly dependent on the interfacial concentration. Hence, our observation of large variations in the latter case are justified.

The effect of the diffusion coefficient on the breakthrough curves for ionic silica is shown in Fig. 15. Different values for ionic conductivity of ionic silica are used for the purpose of simulation. For the base case, we used a value of 50. The other two values are 75 and 30. For a diffusivity of 75, the breakthrough for ionic silica was observed after 38 days. This is lower than the breakthrough for the base case. This is anomalous behavior, because, with an increase in the ionic conductivity, the diffusion coefficient for silica increases. An increase in the diffusion coefficient decreases the Schmidt number, as diffusion coefficient is in the denominator of the formula used for the calculation of the Schmidt number. This should increase the liquid phase mass transfer coefficient. With an increase in the liquid phase mass transfer coefficient, the anionic resin should take in more ionic silica, giving a delayed breakthrough. But, an increase in the diffusivity of silica increases the interfacial concentration. This increase in the interfacial concentration decreases the rate of ion exchange for silica. The decrease in the rate of exchange offsets the increase in the liquid phase mass transfer coefficient. Therefore, we observe an earlier breakthrough with an increase in the diffusivity. The value of ionic conductivity for ionic silica was set at 50 for the base case, as the self-diffusivity of silica was estimated to be approximately $1.3 \times 10^{-5} \text{ cm}^2/\text{s}$ by Wilke-Chang(19).

Colloidal silica is formed in the ion exchange column with time. The concentration of colloidal silica entering into the ion exchange column through service water is set equal to zero. Colloidal silica is assumed to form within the column due to aging. Colloidal silica is formed from amorphous silica by polymerization of the individual silica molecules into long polymeric chains. The rate of polymerization affects the rate of colloidal silica formed in the ion exchanger. The rate of polymerization is a

first order reaction. So, the units for K_p , the rate constant for polymerization, are time^{-1} . The value of K_p used for estimating the amount of colloidal silica generated in the column is 0.05 day^{-1} , for the base. The amount of silica formed for a column operation of 175 days is 0.12 PPM. For the other case where K_p was set equal to 0.10 day^{-1} , the amount of colloidal silica formed was equal to 0.075 PPM or 75 PPB. These two results are shown in Figure 16.

Colloidal silica is formed by the rate of polymerization of amorphous silica and a part of it is hydrolyzed back into amorphous silica, by hydrolysis. The amount of colloidal silica at any instant of time is a net amount of colloidal silica formed in the exchanger due to the rate of polymerization and the removal due to the rate of hydrolysis. Therefore, the rate of hydrolysis is also important in estimating the colloidal silica content at any instant. The rate constant of hydrolysis, K_h , has the same units of rate of polymerization, i.e., time^{-1} . Typical values used in estimating the rate of hydrolysis are 0.15 day^{-1} (for the base case), 0.10 day^{-1} , 0.20 day^{-1} . If K_h equals K_p , then, the amount of colloidal silica formed in the exchanger would be equal to zero. Therefore, that particular case is avoided. The variation in the concentration of colloidal silica with respect to the rate of hydrolysis is shown in Fig. 17.

The selectivity coefficient for monovalent ionic silica over hydroxyl ion is not known precisely. So, different values of randomly chosen selectivity coefficients for monovalent ionic silica were simulated. The results show that the breakthrough for monovalent ionic silica occurred after 45 days, when the selectivity coefficient was equal to 1.0. For a selectivity coefficient of 3.0, the breakthrough was delayed until 85 days.

The value of K_p used for estimating the amount of colloidal silica generated in the column is 0.05 day^{-1} , for the base. The amount of silica formed for a column operation of 175 days is 0.12 PPM. For the other case where K_p was set equal to 0.10 day^{-1} , the amount of colloidal silica formed was equal to 0.075 PPM or 75 PPB. These two results are shown in Figure 16.

Colloidal silica is formed by the rate of polymerization of amorphous silica and a part of it is hydrolyzed back into amorphous silica, by hydrolysis. The amount of colloidal silica at any instant of time is a net amount of colloidal silica formed in the exchanger due to the rate of polymerization and the removal due to the rate of hydrolysis. Therefore, the rate of hydrolysis is also important in estimating the colloidal silica content at any instant. The rate constant of hydrolysis, K_h , has the same units of rate of polymerization, i.e., time^{-1} . Typical values used in estimating the rate of hydrolysis are 0.15 day^{-1} (for the base case), 0.10 day^{-1} , 0.20 day^{-1} . If K_h equals K_p , then, the amount of colloidal silica formed in the exchanger would be equal to zero. Therefore, that particular case is avoided. The variation in the concentration of colloidal silica with respect to the rate of hydrolysis is shown in Fig. 17.

The selectivity coefficient for monovalent ionic silica over hydroxyl ion is not known precisely. So, different values of randomly chosen selectivity coefficients for monovalent ionic silica were simulated. The results show that the breakthrough for monovalent ionic silica occurred after 45 days, when the selectivity coefficient was equal to 1.0. For a selectivity coefficient of 3.0, the breakthrough was delayed until 85 days.

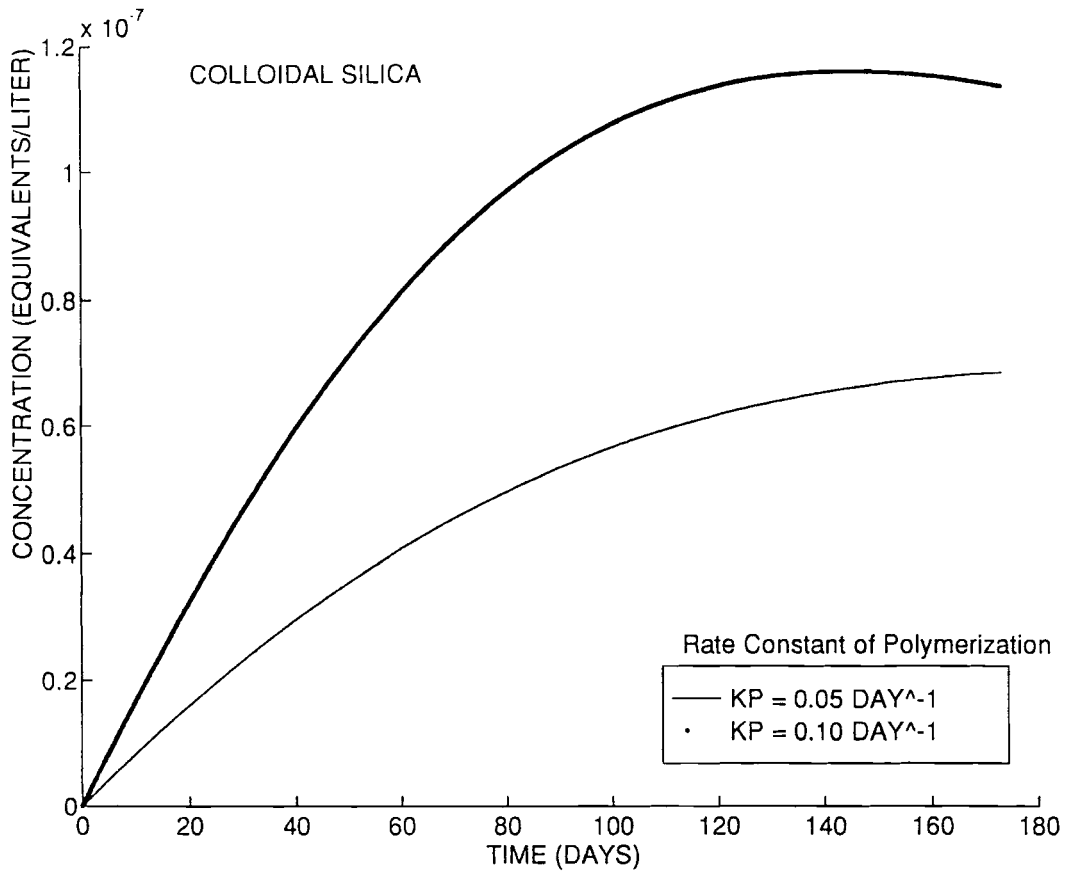


Figure 16. Effect of rate constant for polymerization on silica breakthrough

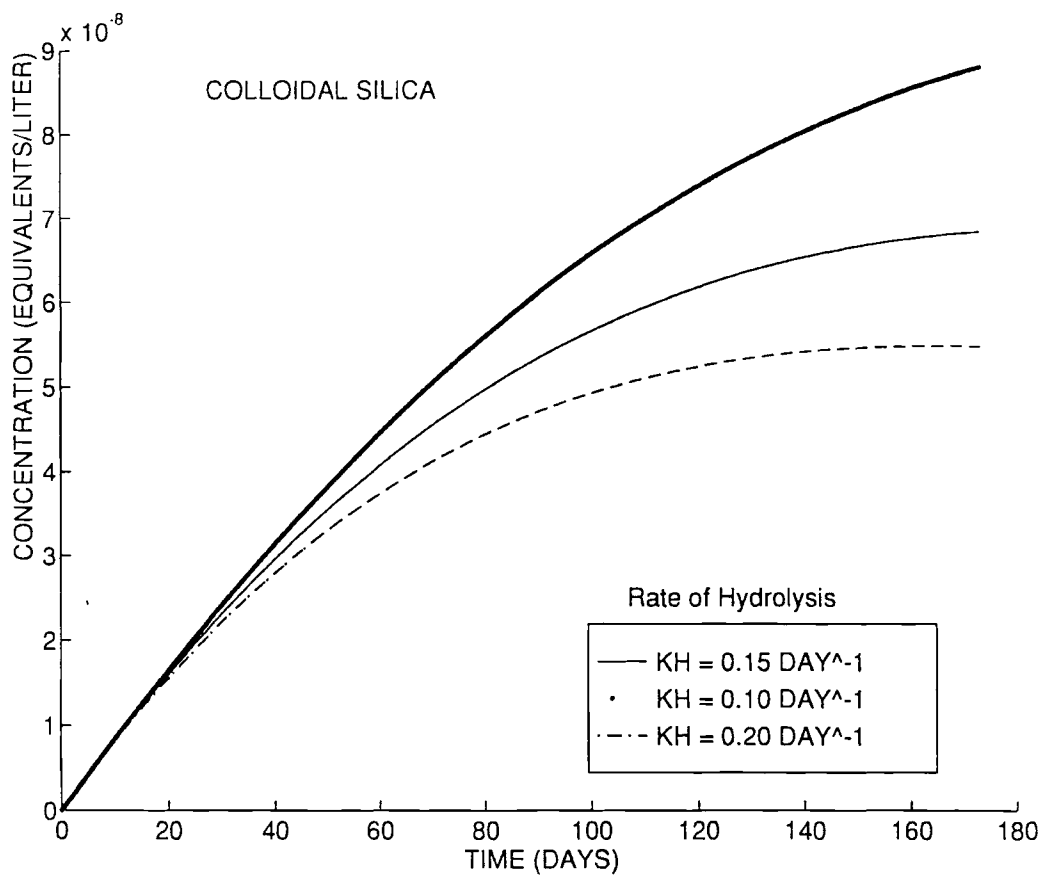


Figure 17. Effect of rate constant for hydrolysis on silica effluent concentrations

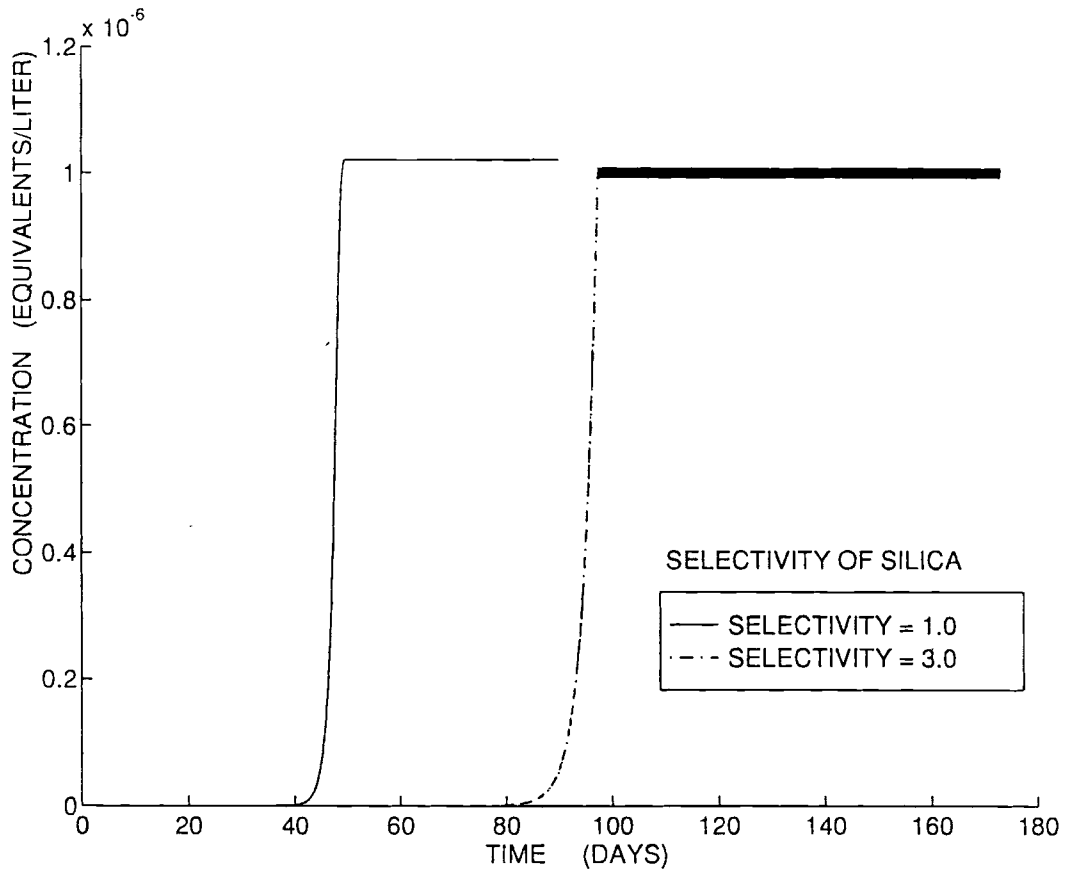


Figure 18. Effect of selectivity coefficient of silica on silica breakthrough

When the selectivity coefficient was set equal to 3.0, we have ionic silica displacing hydroxyl ions in the ion exchanger. Therefore, the hydroxyl ions are pushed further down the column. The band of monovalent ionic silica is seen above the band of hydroxyl ions. This implies that more of monovalent ionic silica is exchanged in preference to the hydroxyl ions. As more silica is taken up by the anionic resin, we see a delayed ionic silica breakthrough. This is what the simulation with a selectivity coefficient of 3.0 shows us in Figure 18. In a case where the selectivity coefficient is lower than 1.0, we expect a much earlier breakthrough.

The effect of initial amount of amorphous silica present in the influent service water on the breakthroughs of particulate, colloidal, and ionic silica can be seen in Figures 19, 20, and 21. Two different cases are considered here. The initial amount of amorphous silica entering into the exchanger for the base case is 15 PPM. Another simulation is run with a value of 30 PPM amorphous silica. The results show that the amount of amorphous silica entering into the mixed bed is not a strong parameter effecting the breakthroughs of particulate, colloidal, and ionic silica.

The concentration of particulate silica produced in the ion exchange column is dependent on the amount of amorphous silica entering into the column and the equilibrium rate constant for eq. (II-5). The value of the rate constant for this reaction is 1.995×10^{-6} , for the base case. The other two cases considered were for rate constant of 1.995×10^{-3} , 1.995×10^{-5} . The variation in the concentration of particulate silica with changes in the equilibrium constant for this reaction can be seen in Figure 22.

The breakthrough curves for all the participating ions in the mixed bed are plotted in Figure 23. The ions that participated are: sodium, potassium, chloride, monovalent ionic silica, hydrogen, and hydroxyl ions. Ionic silica was found to breakthrough earlier than sodium, potassium, and chloride ions. This is because silica is known to form the weakest acid known, silicic acid, which is loosely held onto the anionic resin. Therefore,

silica is the first anion to show up in the effluent water as “silica leakage.” The column conditions are the same as those provided in the base case table (Table II).

The effect of ionic silica feed concentration has a significant impact on the breakthrough curves as seen in Figures 24. The base case was for an inlet silica concentration of 1 PPM. Two other cases are studied here, one at influent concentration of 5 PPM and the other with an influent concentration of 10 PPM. For the first case, silica breakthrough was observed after 45 days. The breakthrough curves for the other two cases are 13 and 8 days, respectively. When the concentration of the ionic silica entering into the ion exchange column increases, we expect more silica to be exchanged onto the anionic resin. This makes the resin lose its capacity rather early. This causes lesser silica to be exchanged on to the anionic resin as the resin is no longer in a position to exchange and has to be regenerated. Therefore, we observe an earlier silica breakthrough.

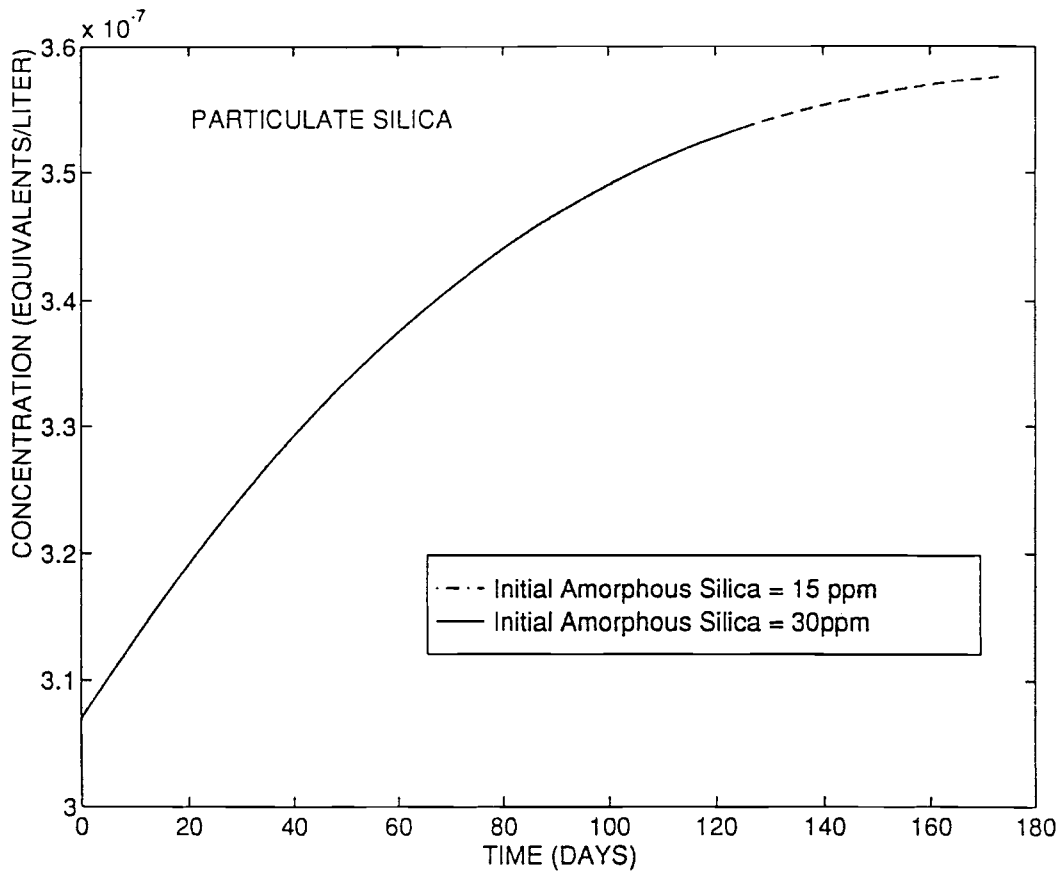


Figure 19. Effect of amorphous silica on particulate silica effluent concentrations

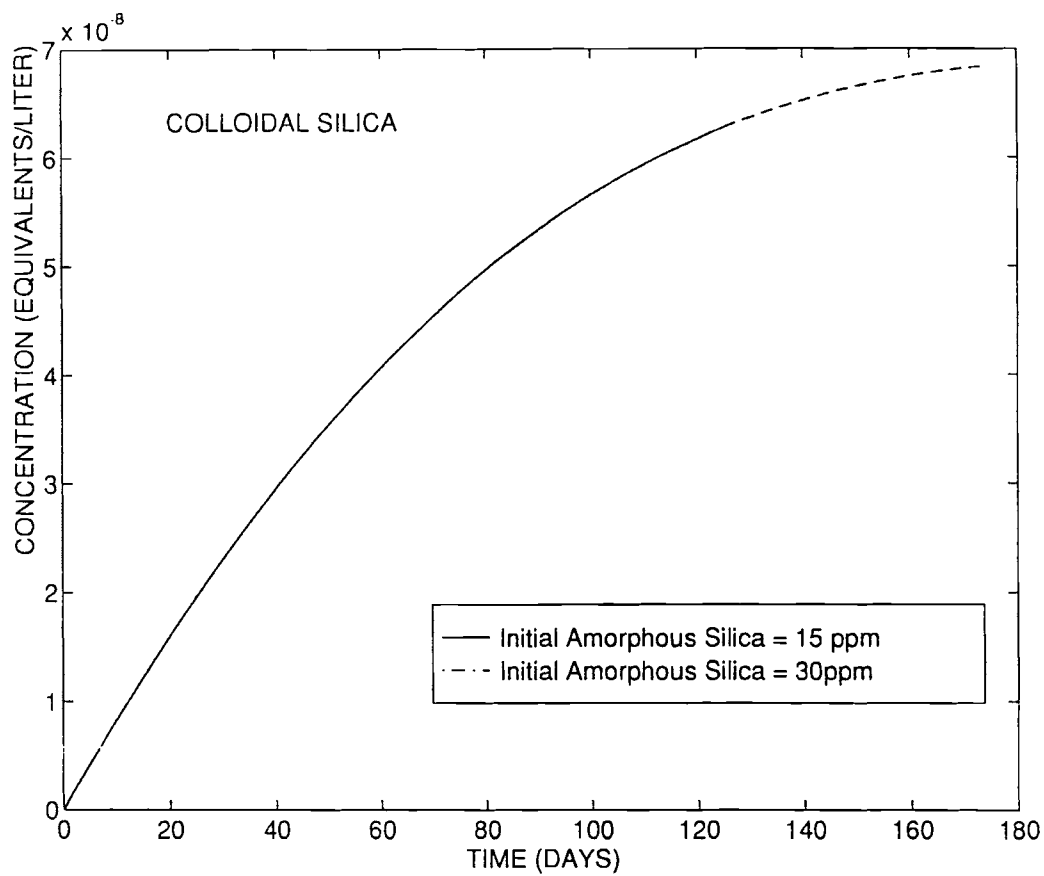


Figure 20. Effect of amorphous silica on colloidal silica breakthrough

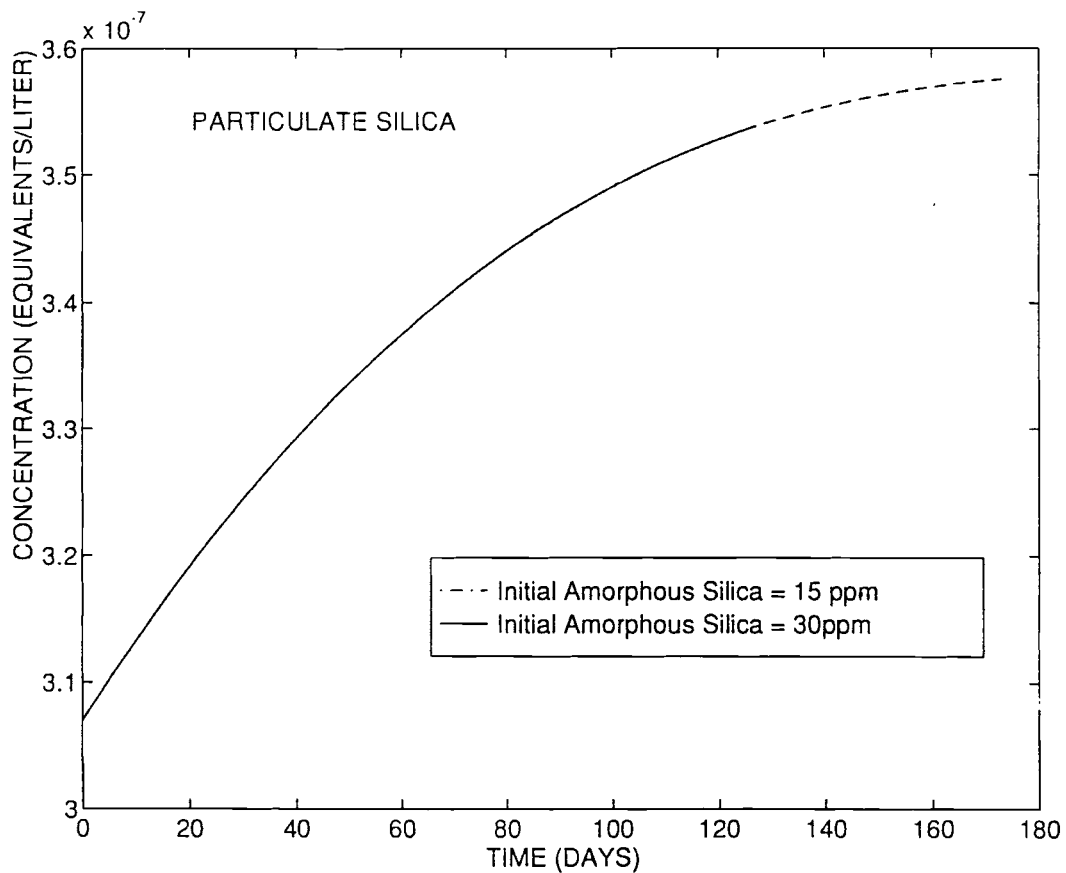


Figure 21. Effect of amorphous silica on particulate silica effluent concentrations

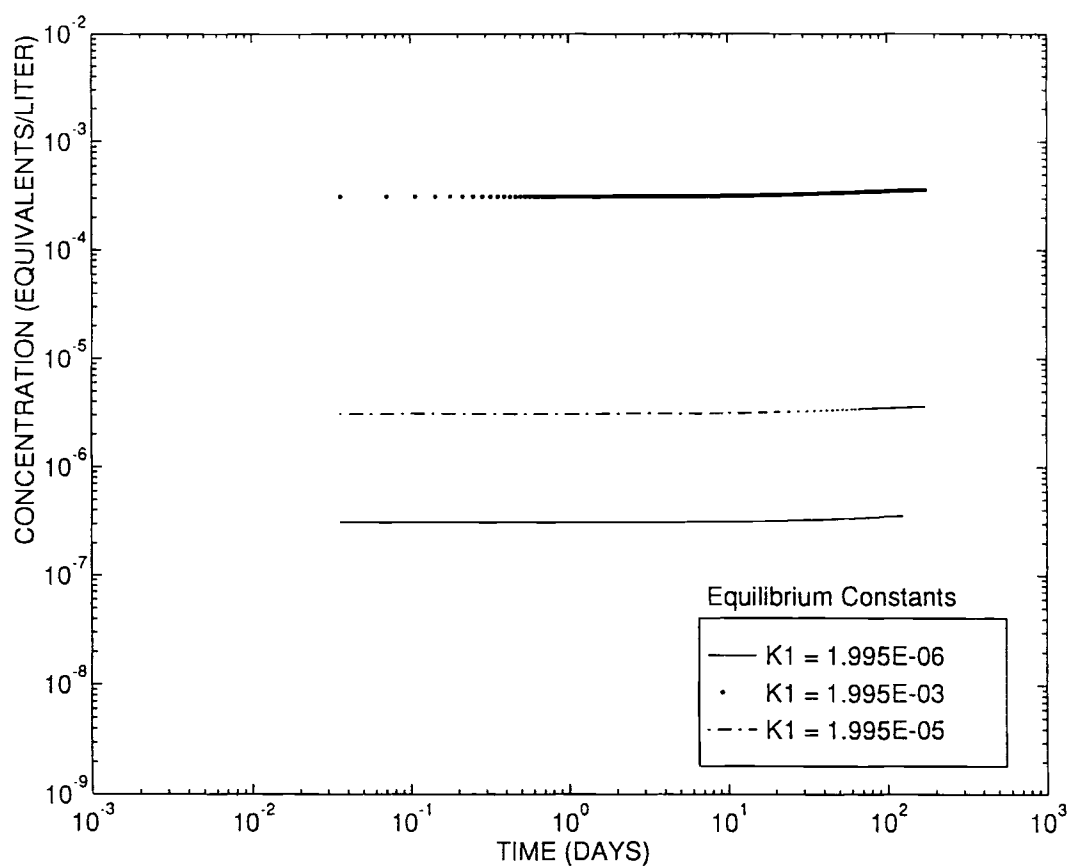


Figure 22. Effect of Equilibrium Constant on particulate silica breakthrough

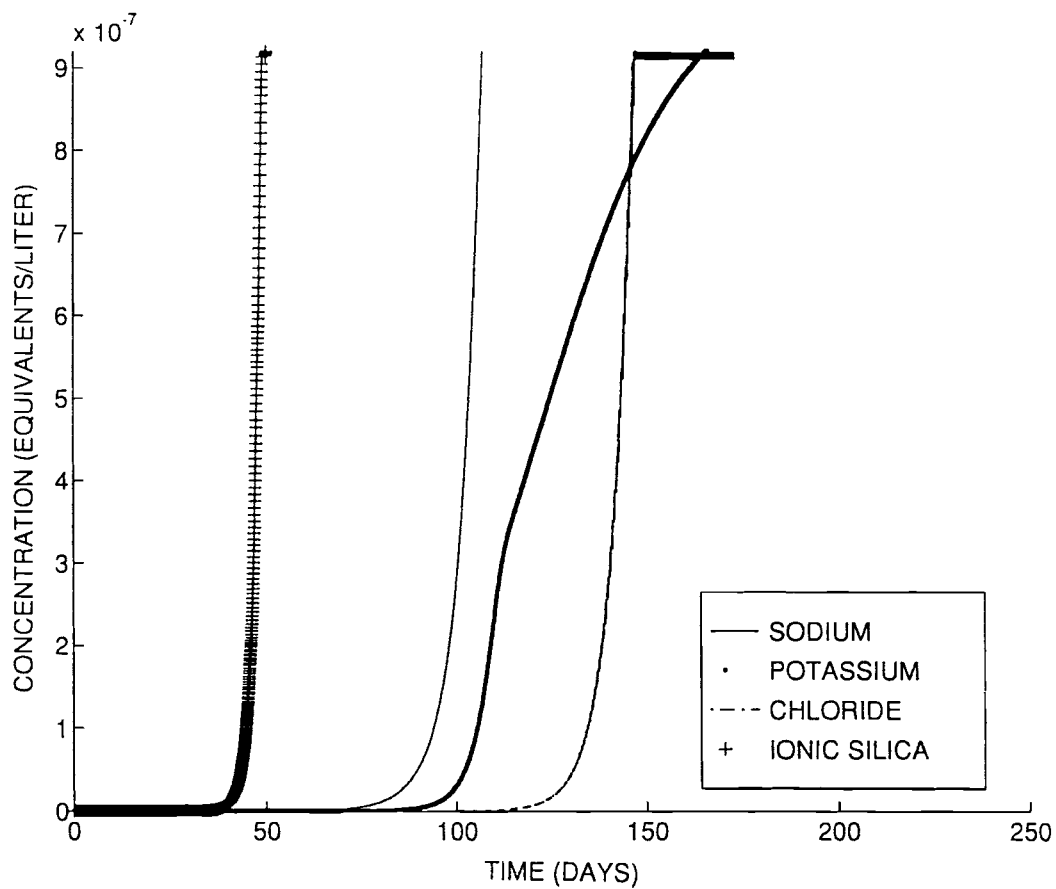


Figure 23. Breakthrough of all the participating ions

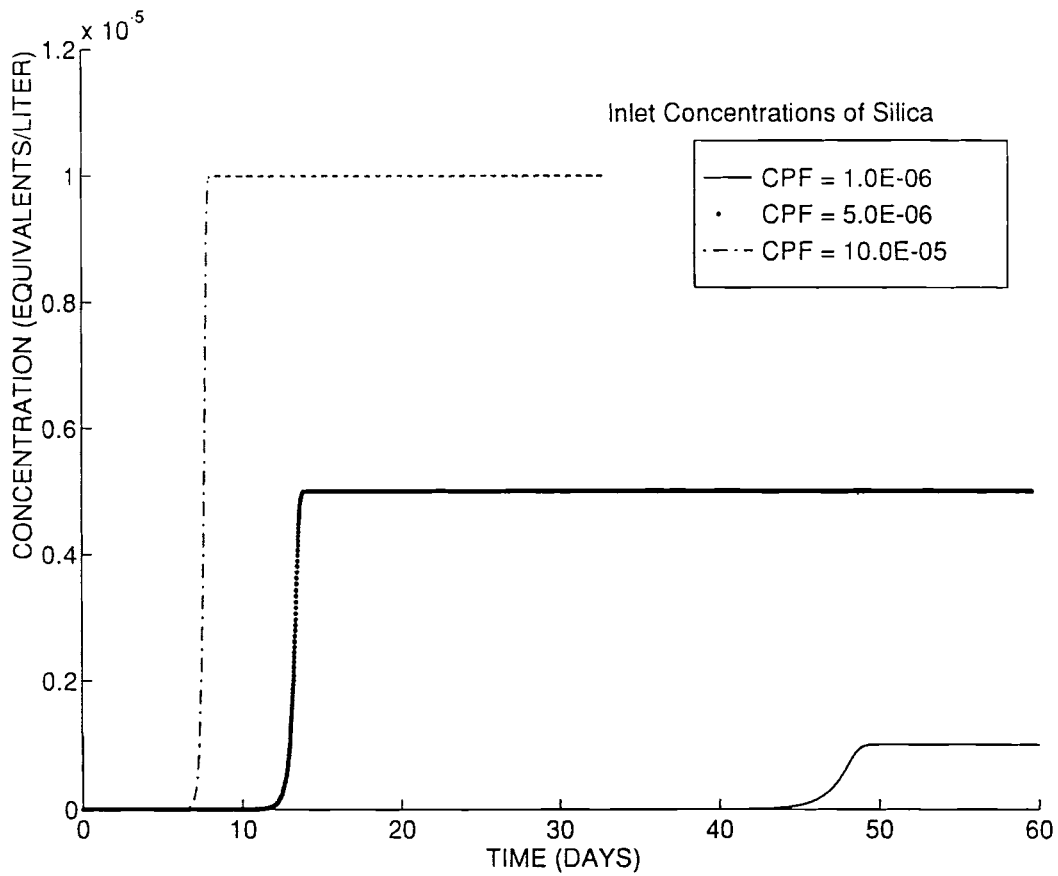


Figure 24. Effect of inlet concentration of ionic silica on silica breakthrough

CHAPTER V

CONCLUSIONS

The model developed in this study deals with a topic which has not received great attention in the past. An equilibrium subroutine was written which accounts for the effect of soluble silica on the concentration of H^+ ions, other than the dissociation constant of water. This subroutine differs from the equilibrium subroutine for ternary exchange developed by Zecchini (1990). A subroutine was developed to predict the interfacial concentrations for monovalent anionic silica where Freundlich equation was used. The model accounts for the removal of ionic, particulate, and colloidal forms of silica. Particle loading of ionic silica on the anionic exchange resin is required at each slice in the mixed bed.

A Freundlich adsorption isotherm was employed to account for particulate adsorption of colloidal and amorphous silica in the bulk liquid phase. This approach gives better results compared to Langmuir adsorption isotherm.

The ternary exchange model was used to predict the outlet concentrations of monovalent anionic silica, chloride, sodium and potassium. Monovalent ionic silica showed earlier breakthrough than other ions. Various parameters that effect the breakthrough of ionic silica were considered and simulations were run to understand their role.

Test simulations were made for a typical industrial ion exchange column. Values of dimensionless time-distance increment (τ) and dimensionless distance

increment(ξ) are 0.002 and 0.004. The model was found to be more sensitive to changes in ξ than to changes in τ . According to Haub (1984), there would be a rapid decrease in the impurity concentrations as the influent moves down the column, but the active exchange zone moves much slowly down the column.

The breakthrough predictions from the model for monovalent ionic silica were in very good agreement with the works of Kataoka and Muto (1993). Most of the predictions were qualitative since little data is available in the literature.

Recommendations

The present model suffers from lack of experimental data on the exchange kinetics of ionic and particulate silica. Experimental data is necessary to evaluate specific performance of ion exchange system with the present model.

The amount of divalent ionic silica produced in the column due to further reaction of monovalent ionic silica, was assumed to be negligible. This assumption is valid for only those operations where the pH of the inlet water is less than 10.7. For higher pH, we need to account for divalent form of ionic silica. The rate equations for a divalent species will be different (Pondugula, 1994).

The effect of temperature on the selectivity coefficients and adsorption isotherms is not known. The values used for coefficients and adsorption indices are approximated at 25⁰ C. Variation of these values with changes in service water temperature has to be determined and incorporated into the model. The temperature effects on other parameters, such as the solution viscosity, diffusivity, water dissociation constant are incorporated in the model.

BIBLIOGRAPHY

- Bajpai, R. K. , Gupta, A. K. and Gopala Rao, M. (1974). Single particle studies of binary and ternary cation exchange kinetics. AICHE J., 20 (5), 989-995.
- Blume, R. (1987). Preparing ultrapure water. Chem. Eng. Prog. (Dec), 55-57.
- Calmon, C. (1986). Recent developments in water treatment by ion exchange. Reactive polymers, 4, 131-146.
- Copeland, J. P., Henderson, C. L. and Marchello, J. M. (1967). Influence of resin selectivity on film diffusion controlled ion exchange. AICHE J., 13, 449-452.
- Divekar, S. V., Foutch, G. L., and Haub, C. E. (1987). Mixed bed ion exchange at concentrations approaching the dissociation of water. Temperature effects. Ind. Eng. Chem. Res., 26(9), 1906-1909.
- Dranoff, J. S. and Lapidus, L. (1961). Ion exchange in ternary systems. Ind. Eng. Chem., 53, 71-76.
- Harries, R. R. (1991). Ion exchange kinetics in ultrapure water systems. J. Chem. Tech. Biotechnol., 51, 437-447.
- Haub, C. E. (1984). M.S. Thesis, Oklahoma State University, Stillwater, OK.
- Haub, C. E. and Foutch, G. L. (1986a). Mixed-bed ion exchange at concentrations approaching the dissociation of water 1. Model development. Ind. Eng. Chem. Fund., 25, 373-381.
- Haub, C. E. and Foutch, G. L. (1986a). Mixed-bed ion exchange at concentrations approaching the dissociation of water 2. Column model applications. Ind. Eng. Chem. Fund., 25, 381-385.
- Helfferich, F. G. (1962). Ion Exchange. McGraw Hill Book Company, New York.

- Helfferrich, F. G. (1984). Conceptual view of column behavior in multicomponent adsorption or ion exchange systems. AICHE Symposium Series, 80, (233), 1-13.
- Helfferrich, F. G. (1990). Models and physical Reality in ion-exchange kinetics. Reactive Polymers, 13, 191-194
- Iler, R. K. (1955). Colloid Chemistry of Silica and silicates. Cornell University Press, Ithaca, N.Y.
- Kataoka, T. and Muto, A. (1991). Removal of Dilute Silicate by Ion Exchange Method-Adsorption Equilibrium Relation of silicate and an OH-type Resin. Proceedings of the International Conference on Ion Exchange. Tokyo, 1991, 329-334.
- Kataoka, T. and Muto, A. (1993). The Removal of Soluble Dilute Silicate from water by Ion Exchange Resins. Proceedings of the Ion-Ex '93 Conference. U.K, 1993, 159-166
- Kataoka, T., Yoshida, H. and uemura T. (1987). Liquid-side ion exchange mass transfer in a ternary system. AICHE J., 33, 202-210.
- Kunin, R. (1960). Elements of ion exchange. Reinhold publishing corporation, N.Y.
- McCartney, B. (1987). Ultrapure water for the silicon chip industry. The Chemical Engineer (Jan.), 24-26.
- Omatete, O. O., Vermeulen, T. and Clazie, R. N. (1980a). Column dynamics of ternary ion exchange. Part I. Diffusion and mass transfer relations. Chem. Engineering J., 19, 229-240.
- Omatete, O. O., Vermeulen, T. and Clazie, R. N. (1980b). Column dynamics of ternary ion exchange. Part II. Solution mass transfer controlling. Chem. Engineering J., 19, 241-250.
- Owens, L. Dean. Practical Principles of Ion Exchange Water Treatment, 1985, Tall Oaks Publishing, inc. NJ.
- Pondugula, S. K. (1994). Mixed bed ion exchange modeling for divalent ions in a ternary system. M.S. thesis, Oklahoma State University, Stillwater, OK.

Sadler, M.A. (1993). Developments in the production and control of ultrapure water.

Ion Exchange Processes: Advances and Applications, 15-28.

Schlogl, R. and Helfferich, F.G. (1957). comment on the significance of diffusion

potentials in ion exchange. J. Chem. Phys., 26, 5-7.

Yoon, T. (1990). Ph.D. Dissertation, Oklahoma State University, Stillwater, OK.

Yoshida, H., and Kataoka, T.,(1987). Intraparticle ion exchange mass transfer in ternary

system. Ind. Eng. Chem., 26, 1179-1184.

Zecchini, E. J. (1990). Solutions to selected problems in multi-component mixed bed ion

exchange modeling. Ph.D. Thesis, Oklahoma State University.

Zecchini, E.J. (1990). M.S. Thesis, Oklahoma State University, Stillwater, OK.

Zecchini, E. J., and Foutch, G. L. (1991). Mixed bed ion-exchange modeling with amine

form cation resins. Ind. Eng. Chem. Res., 30 (8), 1886.

APPENDIX A

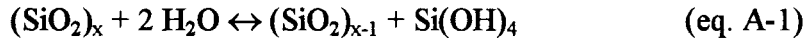
SILICA EQUILIBRIUM

The various forms of silica considered in the model development are:

$[(\text{SiO}_2)_x]$	Amorphous form
$[(\text{SiO}_2)_{x-1}]$	Particulate form
$[\text{Si}(\text{OH})_4]$	Soluble form
$[\text{H}_3\text{SiO}_4^-]$	Monovalent form
$[\text{H}_2\text{SiO}_4^{2-}]$	Divalent form

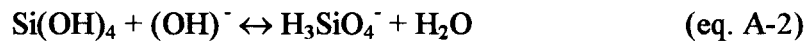
The different reactions considered are given below:

Dissolution:



The equilibrium constant for the above reaction, $K_1 = 1.995 \times 10^{-3}$

Ionization:



The equilibrium constant for the above reaction, $K_2 = 1.85 \times 10^4$

Water Dissociation:



where, K_w is the dissociation constant for water. The water dissociation constant is a function of temperature. Its value at 25°C is 10^{-14} .

The terminology used for each form of silica in the development of the subroutine is given below:

[SX]	Amorphous silica
[SX-1]	Particulate silica
[HS]	Soluble silica
[S ⁻¹]	Monovalent silica
[S ⁻²]	Divalent silica

Applying the electroneutrality in the bulk liquid, we have,

$$[\text{H}^+] + [\text{Na}^+] + [\text{X}^+] = [\text{S}] + [\text{Cl}] + [\text{OH}] \quad (\text{eq. A-4})$$

Applying the mass balance equation for silica in the bulk phase,

$$[\text{SX}] = [\text{SX-1}] + [\text{HS}] \quad (\text{eq. A-5})$$

Equation A-4 can be written as:

$$[\text{H}^+] + \{[\text{Na}^+] + [\text{X}^+] - [\text{Cl}]\} = [\text{S}] + [\text{OH}] \quad (\text{eq. A-6})$$

From Equation A-2, we get,

$$K_2 = [\text{S}][\text{H}_2\text{O}] / \{[\text{HS}][\text{OH}]\} \quad (\text{eq. A-7})$$

Equating the concentration of water to unity (because of its existence in large quantities), the concentration of the monovalent form can be expressed by:

$$[\text{S}] = K_2 [\text{HS}] [\text{OH}] \quad (\text{eq. A-8})$$

Substituting this equation in Equation A-6,

$$[H^+] + \{[Na^+] + [X^+] - [Cl^-]\} = \{K_2 [HS] [OH^-]\} + [OH^-]$$

Using the dissociation constant for water to eliminate $[OH^-]$, and simplifying the resulting equation,

$$[H^+] + \{[Na^+] + [X^+] - [Cl^-]\} = \{K_2 [HS] + 1\}K_w/[H^+] \quad (\text{eq. A-9})$$

Further simplification gives us a quadratic equation in terms of $[H^+]$,

$$[H^+]^2 + \{[Na^+] + [X^+] - [Cl^-]\}[H^+] - \{K_2 [HS] + 1\}K_w = 0 \quad (\text{eq. A-10})$$

The solution for the above quadratic equation is:

$$[H^+] = \{- \{[Na^+] + [X^+] - [Cl^-]\} + \text{sqrt}(\{[Na^+] + [X^+] - [Cl^-]\}^2 + 4 K_w \{K_2 [HS] + 1\})\}/2.0 \quad (\text{eq. A-11})$$

Therefore,

$$[OH^-] = K_w / [H^+]$$

The pH of the solution is obtained from

$$\text{pH} = -\log([H^+])$$

From Equation A-1, Particulate silica can be written as:

$$[SX-1] = K_1 [SX]/[HS] \quad (\text{eq. A-12})$$

Solving Equation A-5, for Particulate silica,

$$[\text{SX-1}] = [\text{SX}] - [\text{HS}] \quad (\text{eq. A-13})$$

Eliminating [SX-1] from the above two equations, we have

$$K_1 [\text{SX}]/[\text{HS}] = [\text{SX}] - [\text{HS}]$$

Simplifying the above equation,

$$[\text{HS}]^2 - [\text{SX}][\text{HS}] + K_1[\text{SX}] = 0 \quad (\text{eq. A-14})$$

The solution of this quadratic equation in [HS] yields

$$[\text{HS}] = \{[\text{SX}] \pm \sqrt{[\text{SX}]^2 - 4 K_1 [\text{SX}]}\}/2.0$$

Therefore, if given [SX], we can calculate $[\text{H}^+]$ using [HS] calculated above and substituting in equation E-11. The new bulk concentration for ionic silica can be obtained from the following equation:

$$[\text{S}] = K_2 [\text{HS}][\text{OH}] \quad (\text{eq. E-15})$$

Similarly, Particulate silica is calculated from Equation A-5

$$[\text{SX-1}] = [\text{SX}] - [\text{HS}] \quad (\text{eq. E-16})$$

The amount of particulate silica adsorbed is determined using Freundlich adsorption isotherm. Similarly, the amount of soluble silica adsorbed can also be

estimated by Freundlich isotherm. Also, divalent form of silica can be seen in the system only if the pH of the solution is higher than 10.7. The reaction for the formation of divalent form of silica from monovalent silica can be written down as:



The rate equation for this reaction is expressed as:

$$[S^-] = K_3 [S] [OH] \quad (\text{eq. A-18})$$

The particulate silica adsorbed onto the resin is determined by Freundlich adsorption isotherms. Mathematically,

$$SXADS = A_x(SX^{xx}B) \quad (\text{eq. A-19})$$

where, SX is the amorphous silica in the service water, SXADS is the adsorbed amorphous silica, A and B are the Freundlich coefficients.

Similar equations can be written for particulate and colloidal silica.

$$PARADS = A_x(PARSIL^{xx}B) \quad (\text{eq. A-20})$$

$$COLADS = A_x(COLSIL^{xx}B) \quad (\text{eq. A-21})$$

where, PARSIL and COLSIL are the amounts of particulate and colloidal silica in service water, PARADS and COLADS are the adsorbed amounts of particulate and colloidal silica, respectively.

Freundlich equation was used to estimate the interfacial concentration of ionic silica.

Mathematically, this can be expressed as:

$$CPI = ((1.0/a_1)^{xx}YP)^{1.0/e_1} \quad (\text{eq. A-22})$$

where, CPI is the interfacial concentration of ionic silica, YP is the particle loading of ionic silica on the anionic resin, a₁ and e₁ are the Freundlich coefficient and Freundlich index, respectively.

APPENDIX B

MODEL PARAMETER VALUES

The various model parameters and their numerical values used for the base case are given below.

Volumetric flow rate: 1.25E5 cm³/s

Fraction of cationic resin 0.4

Fraction of anionic resin 0.6

Cationic particle diameter 0.06 cm

Anionic particle diameter 0.06 cm

Temperature 25^o C

Selectivity coefficient for silica 2.5

Freundlich adsorption coefficient, 1 2.0

(for interfacial concentrations near the resin)

Freundlich adsorption index, 1 0.2

Freundlich adsorption coefficient, 2 2.0

Freundlich adsorption index, 2 4.0

(for bulk phase adsorption of particulates)

Initial concentration of Amorphous silica 15 PPM

Initial resin concentrations:

a)YNO : 0.00001 b) YXO : 0.00001

c)YCO : 0.0001 d) YPO : 0.00001

Initial bulk phase concentrations:

a)CNO : 1PPM b) CXO : 1PPM

c)CCO : 1PPM d) CPO : 1PPM

pH 7.0

KP : 0.05 day⁻¹

KH : 0.15 day⁻¹

(rate constants for the polymerization and hydolysis reactions of colloidal silica)

K1 : 1.995E-03

K2 : 1.85E4

Tau : 0.002

Xi : 0.004

XLAMP : 50

(used for the calculation of diffusivity coefficient for silica)

APPENDIX C

COMPUTER CODE FOR SILICA BREAKTHROUGH

```

*****
* THIS COMPUTER CODE IS DEVELOPED TO *
* SIMULATE THE BREAKTHROUGH CURVES *
* FOR SILICA      [[ SILICA CODE ]]   *
* CODE DEVELOPED BY ZECCHINI, HAUB,   *
* SHARMA PAMARTHY AND Dr. GARY L. FOUTCH *
*****

```

IMPLICIT INTEGER (I-N), REAL*8 (A-H,O-Z)

```

*-----
* Variable and array declaration
*-----

```

```

    REAL KLN, KLX, YNC(4,11000), XNC(4,11000), XXC(4,11000),
  1  RATN(4,11000), YXC(4,11000), RATX(4,11000),
  2  RATC(4,11000), YCA(4,11000), XCA(4,11000),
  3  RATP(4,11000), YPA(4,11000), XPA(4,11000),
  4  KLC, KLP, K1, K2, B2, HS, KP, KH

```

```

*-----
* Function statements for determining non-ionic mass transfer
* coefficients based on system parameters
*-----

```

Carberry's Correlation

$$F1(R,S) = 1.15 * VS / (VD * (S**(2./3.)) * (R**0.5))$$

Kataoka's Correlation

$$1 \quad F2(R,S) = 1.85 * VS * ((VD / (1.-VD))**(1./3.)) / (VD * (S**(2./3.)) * (R**(2./3.)))$$

solubility correlation for amorphous silica

$$F3(p) = 10.**(-2.44 - 0.053 * (p))$$

Initial conditions and bed properties

```

OPEN (9, FILE='s15.d', STATUS='UNKNOWN')
READ(9,*) KPBK, KPPR, TIME
READ(9,*) YNO, YXO, YCO, YPO
READ(9,*) PDC, PDA, VD
READ(9,*) FR, DIA, CHT
READ(9,*) TAU, XI, FCR
READ(9,*) DEN, QC, QA, FAR
READ(9,*) pH, TMP
READ(9,*) CNF, CXF, CCF, CPF
READ(9,*) K1, K2

```

```

READ(9,*) a1, e1, A, B
READ(9,*) XLAMP,SX
READ(9,*) TKCO,TKPO
READ(9,*) KP, KH

```

```

*

```

```

*-----

```

```

* Concentrations and dissociation constant

```

```

*-----

```

```

*

```

```

CP = 1.43123D0+TMP*(0.000127065D0*TMP-0.0241537D0)
ALOGKW = 4470.99/(TMP+273.15)-6.0875+0.01706*(TMP+273.15)

```

```

DISS = 10.**(-ALOGKW)

```

```

CHII = 10.**(-pH)

```

```

COII = DISS/CHII

```

```

CFCAT = CNF+CXF+CHII

```

```

CFANI = CCF+CPF+COII

```

```

IF(ABS(CFCAT-CFANI).LE.(CFCAT/1000.)) GO TO 600

```

```

IF(CFCAT.GT.CFANI) THEN

```

```

WRITE(6,550)

```

```

550 FORMAT(30X,'TOTAL CATIONS IS GREATER THAN TOTAL ANIONS')
GO TO 570

```

```

ELSE

```

```

WRITE(6,560)

```

```

560 FORMAT(30X,'TOTAL ANIONS IS GREATER THAN TOTAL CATIONS')
ENDIF

```

```

570 WRITE(6,580)COII, CHII

```

```

580 FORMAT(30X,'COII =',E10.5,3X,'CHII =',E10.5)

```

```

600 CONTINUE

```

```

IF(CFCAT.GE.CFANI) THEN

```

```

CF = CFCAT

```

```

ELSE

```

```

CF = CFANI

```

```

ENDIF

```

```

*

```

```

*-----

```

```

* Calculate ionic diffusion coefficients based on temperature
* using limiting ionic conductivities (Robinson and Stokes, 1959)

```

```

*-----

```

```

*

```

```

RTF = (8.931D-10)*(TMP+273.16)

```

```

XLAMH = 221.7134+5.52964*TMP-0.014445*TMP*TMP

```

```

XLAMX = 1.40549*TMP+39.1537

```

```

XLAMN = 23.00498+1.06416*TMP+0.0033196*TMP*TMP

```

```

XLAMO = 104.74113+3.807544*TMP

```

```

XLAMC = 39.6493+1.39176*TMP+0.0033196*TMP*TMP

```

DN = RTF*XLAMN
 DX = RTF*XLAMX
 DO = RTF*XLAMO
 DC = RTF*XLAMC
 DH = RTF*XLAMH
 DP = RTF*XLAMP

*

*-----

*Calculate Reynolds and Schmidt numbers and non-ionic
 *mass transfer coefficients

*-----

*

AREA = 3.1415927*(DIA**2)/4.
 VS = FR/AREA
 REC = PDC*100.*VS*DEN/((1.-VD)*CP)
 REA = PDA*100.*VS*DEN/((1.-VD)*CP)
 SCX = (CP/100.)/DEN/DX
 SCN = (CP/100.)/DEN/DN
 SCC = (CP/100.)/DEN/DC
 SCP = (CP/100.)/DEN/DP
 IF (REC.LT.20.) THEN
 KLN = F2(REC,SCN)
 KLX = F2(REC,SCX)
 ELSE
 KLN = F1(REC,SCN)
 KLX = F1(REC,SCX)
 ENDIF
 IF (REA.LT.20.) THEN
 KLC = F2(REA,SCC)
 KLP = F2(REA,SCP)
 ELSE
 KLC = F1(REA,SCC)
 KLP = F1(REA,SCP)
 ENDIF

*

* Calculate the amount of Amorphous Silica initially present

*

* SX = F3(pH)

*

* Calculate total number of steps in distance (NT) down column

*

CHTD = KLC*(1.-VD)*CHT/(VS*PDA)
 write(6,45) CHTD

45 FORMAT(30X,'VALUE OF CHTD IS =',F7.3)

NT = CHTD/XI

*-----
 *Print system parameters and calculated parameters
 *-----

WRITE (6,10)
 WRITE (6,11)
 WRITE (6,12) YNO,YXO
 WRITE (6,86) YCO,YPO
 WRITE (6,13) PDC,PDA,VD
 WRITE (6,14) QC,QA,FCR,FAR
 WRITE (6,15) FR,DIA,CHT
 WRITE (6,89) CNF,CXF
 WRITE (6,90) CCF,CPF,pH
 WRITE (6,92) XLAMP, SX
 WRITE (6,94) TKCO, TKPO
 WRITE (6,95) KP, KH
 WRITE (6,16) DEN,TMP
 WRITE (6,17) TAU,XLNT
 WRITE (6,91) a1,e1,A,B
 WRITE (6,18)
 WRITE (6,19)
 WRITE (6,20)
 WRITE (6,22) REC,KLN
 WRITE (6,88) KLX,KLC
 WRITE (6,23) VS,CP,CF
 WRITE (6,80)
 WRITE (6,81) DX,DN,DH
 WRITE (6,82) DO,DC,DP

*
 *-----
 * Print breakthrough curve headings
 *-----

*
 IF (KPBK.NE.1) GO TO 50
 * WRITE (6,24)
 * WRITE (6,25)
 * WRITE (6,26)
 * WRITE (6,27)
 * WRITE (6,28)
 50 CONTINUE

*-----
 *Print concentration profile headings
 *-----

T = 0.
 TAUPR = KLC*CF*(TIME*60.)/(PDA*QA)
 IF (KPPR.NE.1) GO TO 60


```

WRITE (6,30)
WRITE (6,31) TIME
WRITE (6,32)
WRITE (6,33)
WRITE (6,34)
60  CONTINUE

```

```

*-----
*Set initial resin loading throughout the entire column
*-----

```

```

      MT = NT + 1
      DO 100 M=1,MT
      YNC(1,M)=YNO
      YXC(1,M)=YXO
      YCA(1,M)=YCO
      YPA(1,M)=YPO
100  CONTINUE

```

```

*-----
* Calculate dimensionless program time limit
* based on inlet conditions (at Z=0)
*-----

```

```

      TMAXC = QC*3.142*(DIA/2.)**2.*CHT*FCR/(FR*CF*60.)
      TMAXA = QA*3.142*(DIA/2.)**2.*CHT*FAR/(FR*CF*60.)
      TMAX = MAX(TMAXC,TMAXA)
      TAUMAX = KLC*CF*(TMAX*60.)/(PDA*QA)
      TMAX = TMAX/1440.
      WRITE(6,222)
      WRITE(6,223)TMAX
      WRITE(6,224)
222  FORMAT(' Program run time is based on total resin capacity')
223  FORMAT(' and flow conditions. The program will run for',F12.1)
224  FORMAT(' days of column operation for the current conditions.')

```

```

*-----
* Initialize values prior to iterative loops
*-----

```

```

      J = 1
      JK = 1
      TAUTOT = 0.
      JFLAG = 0
      XNC(JK,NT) = 0.
      KK = 1
      KPRINT = 1000
      SXADS = 0.0
      PARADS = 0.0
      COLADS = 0.0

```

```

*
*-----
*   Time stepping loop within which all column calculations are
*   implemented, time is incremented and outlet concentrations checked
*-----
1  CONTINUE
   IF (TAUTOT.GT.TAUMAX) GOTO 138
*
*   Correction of time step value for Adams-Bashforth Method
*
   IF (J.EQ.4) THEN
       JD = 1
   ELSE
       JD = J + 1
   ENDIF
*-----
*   Set inlet liquid phase fractional concentrations for each
*   species in the matrix
*-----
   XNC(J,1) = CNF/CF
   XXC(J,1) = CXF/CF
   CHO = CHII
   COO = COII
   XCA(J,1) = CCF/CF
   XPA(J,1) = CPF/CF
*-----
*   Loop to increment distance (bed length) at a fixed time
*-----
   DO 400 K=1,NT
*-----
*   Define bulk phase concentrations for subroutines
*-----
   CXO = XXC(J,K)*CF
   CNO = XNC(J,K)*CF
   CCO = XCA(J,K)*CF
   CPO = XPA(J,K)*CF
   CCT2 = CCO
   CNT2 = CNO
   CXT2 = CXO
   CPT2 = CPO
   CH1 = CHO
   CO1 = COO
   YN = YNC(J,K)
   YX = YXC(J,K)
   YC = YCA(J,K)

```

YP = YPA(J,K)

*-----
 *Integrate X using Adams-Bashforth method

*-----
 XXL = XXC(J,K)
 XNL = XNC(J,K)
 XPL = XPA(J,K)
 XCL = XCA(J,K)

*-----
 *Call subroutines to calculate RN, RX, CNI, CXI

*-----
 IF (YX .LT. 1.0) THEN
 IN = 0
 CALL CR (IN,CHO,CNO,CXO,DH,DN,DX,YN,YX,CNI,CXI,RN,RX)
 XXI = CXI/CF
 XNI = CNI/CF
 ELSE
 XXI = 1.0
 XNI = 0.0
 RN = 0.0
 RX = 0.0
 ENDIF

*
 IF (YP .LT. 1.0) THEN
 IN = 1
 CALL AR (IN,TKCO,TKPO,COO,CCO,CPO,DO,DC,DP,
 1 YC,YP,CCI,CPI,RC,RP,a1,e1)
 XCI = CCI/CF
 XPI = CPI/CF
 ELSE
 XPI = 1.0
 XCI = 0.0
 RC = 0.0
 RP = 0.0
 ENDIF

*-----
 *Evaluate the particle rate of exchange

*-----
 RATEN = 6.*RN*(XNL - XNI)*KLN/KLC*PDA/PDC
 RATEX = 6.*RX*(XXL - XXI)*KLX/KLC*PDA/PDC
 RATEC = 6.*RC*(XCL-XCI)
 RATEP = 6.*RP*(XPL - XPI)*KLP/KLC

*
 *First step calculation across the bed inlet

*

```

IF (K .EQ. 1) THEN
RATN(J,1) = RATEN
RATX(J,1) = RATEX
RATC(J,1) = RATEC
RATP(J,1) = RATEP

```

*

*Calculate next time particle loading

*

```

YNC(JD,1) = YNC(J,1)+TAU*RATN(J,1)*QA/QC
YXC(JD,1) = YXC(J,1)+TAU*RATX(J,1)*QA/QC
YCA(JD,1) = YCA(J,1)+TAU*RATC(J,1)
YPA(JD,1) = YPA(J,1)+TAU*RATP(J,1)

```

*

*Check that values are within bounds

*

```

IF(YXC(JD,1)+YNC(JD,1) .GT. 1.0) THEN
CALL CORRECT(YXC(JD,1),YNC(JD,1),YXC(J,1),YNC(J,1),TAU,
RATEX,RATEN)
RATX(J,1) = RATEX*QC/QA
RATN(J,1) = RATEN*QC/QA
ENDIF
IF(YCA(JD,1)+YPA(JD,1) .GT. 1.0)THEN
CALL CORRECT(YCA(JD,1),YPA(JD,1),YCA(J,1),YPA(J,1),TAU,
1 RATEC,RATEP)
RATC(J,1) = RATEC
RATP(J,1) = RATEP
ENDIF
ENDIF

```

*

* -----
* Impliment implicit portion of the GEARS BACKWARD DIFFERENCE method
* from the previous function values. For the first three steps
* use fourth-order Runge Kutta

*

```

IF (K.LE.3) THEN
F1N=XI*6.*RN*(XNC(J,K)-XNI)*FCR*KLN/KLC
F2N=XI*6.*RN*((XNC(J,K)+F1N/2.)-XNI)*FCR*KLN/KLC
F3N=XI*6.*RN*((XNC(J,K)+F2N/2.)-XNI)*FCR*KLN/KLC
F4N=XI*6.*RN*(XNC(J,K)+F3N-XNI)*FCR*KLN/KLC
XNC(J,K+1) = XNC(J,K) - (F1N+2.*F2N+2.*F3N+F4N)/6.
F1X=XI*6.*RX*(XXC(J,K)-XXI)*FCR*KLX/KLC
F2X=XI*6.*RX*((XXC(J,K)+F1X/2.)-XXI)*FCR*KLX/KLC
F3X=XI*6.*RX*((XXC(J,K)+F2X/2.)-XXI)*FCR*KLX/KLC
F4X=XI*6.*RX*(XXC(J,K)+F3X-XXI)*FCR*KLX/KLC
XXC(J,K+1) = XXC(J,K) - (F1X+2.*F2X+2.*F3X+F4X)/6.
F1C=XI*6.*RC*(XCA(J,K)-XCI)*FAR*PDC/PDA

```

```

F2C=XI*6.*RC*((XCA(J,K)+F1C/2.)-XCI)*FAR*PDC/PDA
F3C=XI*6.*RC*((XCA(J,K)+F2C/2.)-XCI)*FAR*PDC/PDA
F4C=XI*6.*RC*(XCA(J,K)+F3C-XCI)*FAR*PDC/PDA
XCA(J,K+1) = XCA(J,K) - (F1C+2.*F2C+2.*F3C+F4C)/6.
F1P=XI*6.*RP*(XPA(J,K)-XPI)*FAR*KLP/KLC*PDC/PDA
F2P=XI*6.*RP*((XPA(J,K)+F1P/2.)-XPI)*FAR*KLP/KLC*PDC/PDA
F3P=XI*6.*RP*((XPA(J,K)+F2P/2.)-XPI)*FAR*KLP/KLC*PDC/PDA
F4P=XI*6.*RP*(XPA(J,K)+F3P-XPI)*FAR*KLP/KLC*PDC/PDA
XPA(J,K+1) = XPA(J,K) - (F1P+2.*F2P+2.*F3P+F4P)/6.

```

```
ELSE
```

```

COEN = 3./25.*XNC(J,K-3)-16./25.*XNC(J,K-2)+
1 36./25.*XNC(J,K-1)-48./25.*XNC(J,K)
XNC(J,K+1) = -(XI*12./25.)*FCR*RATN(J,K)-COEN
COEX = 3./25.*XXC(J,K-3)-16./25.*XXC(J,K-2)+
1 36./25.*XXC(J,K-1)-48./25.*XXC(J,K)
XXC(J,K+1) = -(XI*12./25.)*FCR*RATX(J,K)-COEX
COEC = 3./25.*XCA(J,K-3)-16./25.*XCA(J,K-2)+
1 36./25.*XCA(J,K-1)-48./25.*XCA(J,K)
XCA(J,K+1) = -(XI*12./25.)*FAR*RATC(J,K)-COEC
COEP = 3./25.*XPA(J,K-3)-16./25.*XPA(J,K-2)+
1 36./25.*XPA(J,K-1)-48./25.*XPA(J,K)
XPA(J,K+1) = -(XI*12./25.)*FAR*RATP(J,K)-COEP
ENDIF

```

```
*
```

```

-----
* Determine concentrations for next distance step and recalculate
* bulk phase equilibria

```

```
*
```

```

-----
CXO = XXC(J,K+1) * CF
CNO = XNC(J,K+1) * CF
CCO = XCA(J,K+1) * CF
CPO = XPA(J,K+1) * CF
CHO = CH1-CNO-CXO+CXT2+CNT2
COO = CO1-CCO+CCT2-CPO+CPT2

```

```
*
```

```

-----
* SILICA EQUILIBRIUM

```

```
*
```

```

-----
SXADS = SXADS + A*(SX**B)
SX = SX-SXADS
B1 = SX**2.0
C1 = K1*SX
D1 = ABS(B1-4.0*C1)
IF(D1 .LT. 0.0) D1 = 0.0
HS = ABS(SX-SQRT(D1))/2.0
COLSIL = SX*KP/(ABS(KH-KP))*(EXP(-KP*TAUTOT)-EXP(-KH*TAUTOT))
SX = ABS(SX-COLSIL)

```

```

PARSIL = ABS(SX-COLSIL)
PARADS = PARADS+A*(PARSIL**B)
PARSIL = (PARSIL-PARADS)
COLADS = A*(COLSIL**B)
COLSIL = COLSIL-COLADS
TOTADS = SXADS + PARADS + COLADS
TOTSIL = PARSIL + CPO + HS + COLSIL

```

*

* Particulate Silica for this step is the amorphous silica for the next step

*

```
CALL EQB(DISS,CNO,CXO,CCO,CPO,COO,CHO,K2,HS)
```

*

```

YX = YXC(J,K+1)
YN = YNC(J,K+1)
YC = YCA(J,K+1)
YP = YPA(J,K+1)

```

*

* -----
* Determine rates at constant xi for solution of the tau
* material balance

*

```

IF (YX.LT.1.0) THEN
  IN = 0
  CALL CR (IN,CHO,CNO,CXO,DH,DN,DX,YN,YX,CNI,CXI,RN,RX)
  XXI = CXI/CF
  XNI = CNI/CF
ELSE
  XXI = 1.0
  XNI = 0.0
  RN = 0.0
  RX = 0.0
ENDIF

```

*

```

IF (YP.LT.1.0) THEN
  IN = 1
  CALL AR(IN,TKCO,TKPO,COO,CCO,CPO,DO,DC,DP,
1      YC,YP,CCI,CPI,RC,RP,a1,e1)
  XCI = CCI/CF
  XPI = CPI/CF
ELSE
  XPI = 1.0
  XCI = 0.0
  RP = 0.0
  RC = 0.0
ENDIF

```

*

```

RATN(J,K+1) = 6.*RN*((XNC(J,K+1)) - XNI)*KLN/KLC*PDA/PDC
RATX(J,K+1) = 6.*RX*((XXC(J,K+1)) - XXI)*KLX/KLC*PDA/PDC
RATC(J,K+1) = 6.*RC*((XCA(J,K+1))-XCI)
RATP(J,K+1) = 6.*RP*((XPA(J,K+1))-XPI)*KLP/KLC + XPL*(YPOL-YP)

```

```

* -----
* Integrate Y using Adams-Bashforth (calculate next particle loading)
* -----

```

```

YNC(JD,K+1) = YNC(J,K+1) + TAU*RATN(J,K+1)*QA/QC
YXC(JD,K+1) = YXC(J,K+1) + TAU*RATX(J,K+1)*QA/QC
YCA(JD,K+1) = YCA(J,K+1) + TAU*RATC(J,K+1)
YPA(JD,K+1) = YPA(J,K+1) + TAU*RATP(J,K+1)

```

```

* -----
* Check values within bounds
* -----

```

```

IF ((YNC(JD,K+1)+YXC(JD,K+1)).GT.1.0) THEN
  CALL CORRECT(YXC(JD,K+1),YNC(JD,K+1),YXC(J,K+1),YNC(J,K+1),TAU,
1          RATX(J,K+1),RATN(J,K+1))
  RATX(J,K+1) = RATX(J,K+1)*QC/QA
  RATN(J,K+1) = RATN(J,K+1)*QC/QA
ENDIF
IF ((YPA(JD,K+1)+YCA(JD,K+1)).GT.1.0) THEN
  CALL CORRECT(YCA(JD,K+1),YPA(JD,K+1),YCA(J,K+1),YPA(J,K+1),TAU,
1          RATC(J,K+1),RATP(J,K+1))
ENDIF

```

```

* -----
* Print concentration profiles
* -----

```

```

IF (KPPR.NE.1) GO TO 350
IF (TAUTOT.LT.TAUPR) GO TO 350
JFLAG = 1
ZA = FLOAT(NT)
ZB = FLOAT(K-1)
Z = ZB*CHT/ZA
KOUNT = KOUNT+1
IF (KOUNT.NE.(KOUNT/10*10)) GOTO 350

```

```

* -----
* Open data file
* -----

```

```

c OPEN (6, FILE='NEWMUL6.DAT', STATUS='UNKNOWN')
c WRITE (6,35) Z,XNC(J,K),XXC(J,K),YNC(J,K),YXC(J,K)
c CLOSE (6)

```

```

350 CONTINUE
400 CONTINUE

```

```

* -----
* Print breakthrough curves

```

```

* -----
  IF (KPBK.NE.1) GOTO 450
*   write(*,137)
* 137 format(' TIME(MIN)',8X,'SODIUM',8X,'AMINE',7X,'CHLORIDE',
*   1      7X,'2ND ANION',6X,'pH')
      TAUTIM = TAUTOT*PDA*QA/(KLC*CF*60.)/1440.
      pH=14.+LOG10(COO)
      WRITE(6,139) TAUTIM,CNO,CXO,CCO,CPO,pH
139  FORMAT(1x,F9.3,2x,E12.5,4X,E12.5,3x,E12.5,3x,E12.5,2x,F6.3)
* -----
* Store every tenth iteration to the print file
* -----
      IF(KPRINT.NE.1000) GOTO 500
      KPRINT=0
* -----
* Open data file
* -----
*   WRITE (*,29) TAUTIM,CNO,CXO,CCO,CPO,pH
450 IF(KPBK .NE. 2) GO TO 500
      TAUTIM = TAUTOT*PDA*QA/(KLC*CF*60.)
      WRITE(6,145) SX,PARSIL,HS,CPO,TOTADS,TOTSIL
145  FORMAT(1x,F9.3,2x,E12.5,4X,E12.5,3x,E12.5,E12.5,E12.5)
* -----
* Store every tenth iteration to the print file
* -----
      IF(KPRINT.NE.1000) GOTO 500
      KPRINT=0
500 CONTINUE
      KPRINT=KPRINT+1
      KK = KK+1
      JK = J
      IF (J.EQ.4) THEN
          J = 1
      ELSE
          J = J+1
      ENDIF
* -----
* End of loop, return to beginning and step in time
* -----
      IF (JFLAG.EQ.1) STOP
      TAUTOT = TAUTOT + TAU
      GOTO 1
* -----
* .....printout formats.....
* -----

```



```

10 FORMAT (' MIXED BED SYSTEM PARAMETERS')
11 FORMAT (' -----')
12 FORMAT (' RESIN REGENERATION',3X,': YNO =',F7.5,6X,'YXO =',F7.5)
86 FORMAT (25X,'YCO =',F7.5,6X,'YPO =',F7.5)
13 FORMAT (' RESIN PROPERTIES',8X,'PDC =',F6.4,'cm',5X,'PDA =',F6.4,
1      'cm',7X,'VD =',F5.3)
14 FORMAT (' RESIN CONSTANTS(eq/l): QC =',F5.3,3X,'QA =',F5.3,3X,
1      'FCR =',F5.3,3X,'FAR =',F5.3)
15 FORMAT (25X,'FR =',F9.1,' ml/s',2X,'DIA =',F6.1,
1      ' cm',4X,'CHT =',F6.1,' cm')
16 FORMAT (25X,'DEN =',F6.4,'g/ml',5X,'TEMP =',F4.1,' C')
80 FORMAT (' DIFFUSIVITIES :')
81 FORMAT (25X,'DX =',E10.4,2X,'DN =',E10.4,2X,'DH =',E10.4)
82 FORMAT (25X,'DO =',E10.4,2X,'DC =',E10.4,2X,'DP =',E10.4)
17 FORMAT (' INTEGRATION INCREMENTS: TAU =',F7.5,8X,'XI =',F7.5,
1      6X,'NT =',I6)
18 FORMAT (' ')
19 FORMAT (' CALCULATED PARAMETERS')
20 FORMAT (' -----')
22 FORMAT (' TRANSFER COEFFICIENTS: REC =',E9.4,' KLN =',E9.4)
23 FORMAT (' SUPERFICIAL VELOCITY:',2X,'VS =',F7.3,' cm/s',2X,
1      ' VISCOSITY =',F7.5,' cp', ' CF =',F10.8)
88 FORMAT (25X,'KLX =',E9.4,' KLA =',E9.4)
89 FORMAT (' INPUT CONCENTRATIONS :',2X,'CNF =',F9.7,6X,'CXF =',F9.7)
90 FORMAT (25X,'CCF =',F9.7,6X,'CPF =',F10.8,3X,'pH =',F5.2)
91 FORMAT (' MODEL PARAMETERS   : a1=',F5.3,2X,'e1=',F4.3,4X,
1      'A=',F4.2,4X,'B=',F4.2)
92 FORMAT (25X,'XLAMP =',F5.2,6X,' SX =',F9.7)
* 93 FORMAT (25X,'TKNH =',F5.2,8X,' TKXH =',F5.2)
94 FORMAT (25X,'TKCO =',F5.2,8X,' TKPO =',F5.2)
95 FORMAT (25X,'KP =',F5.2,11X,'KH =',F5.2)
24 FORMAT (' ')
25 FORMAT (' BREAKTHROUGH CURVE RESULTS:')
26 FORMAT (' -----')
27 FORMAT (' ',5X,'T(MIN)',6X,'SODIUM',6X,'2ND CAT',7X,'CHLORIDE',4X,
1      'SILICA',7X,'pH')
28 FORMAT (' ')
* 29 FORMAT (' ',5(4X,E8.3),5X,F4.2)
30 FORMAT (' ')
31 FORMAT (' CONCENTRATION PROFILES AFTER ',F5.0,' MINUTES')
32 FORMAT (' ')
33 FORMAT (' ',5X,'Z',7X,'XNC',7X,'XXC',7X,'YNC',
1      7X,'YCA')
34 FORMAT (' ')
35 FORMAT (' ',6(2X,E8.3))

```

```

CLOSE (6)
138 STOP
END
*
SUBROUTINE CR (IN,CHO,CNO,CXO,DH,DN,DX,YN,YX,CNI,CXI,RN,RX)
*
* Subroutine to calculate cation rates for ternary exchange
*
IMPLICIT REAL*8 (A-H,O-Z)
INTEGER IN

IF (IN.NE.1) THEN
TKNH = 1.5
TKXH = 2.4
TKNX = TKNH/TKXH
ELSE
TKNH = 15.
TKXH = 4.6
TKNX = TKNH/TKXH
ENDIF
AH = DH/DN
AX = DX/DN
CTO = CNO+CXO+CHO
S = (CHO+CNO+CXO)*(AH*CHO+CNO+AX*CXO)
*
DENOM1 = TKNH+(1-TKNH)*YN+(TKNX-TKNH)*YX
DENOM2 = AH*TKNH+(1-AH*TKNH)*YN+(AX*TKNX-AH*TKNH)*YX
*
* Calculate Interfacial Concentrations
*
CNI = YN*(S/DENOM1/DENOM2)**0.5
IF (CNI.LE.0.0) CNI=0.0
CXI = CNI*TKNX*YX/YN
IF (CXI.LE.0.0) CXI=0.0
CHI = CNI*TKNH*(1-YN-YX)/YN
IF (CHI.LE.0.0) CHI=0.0
CTI = CNI+CHI+CXI
CNR = CNI/CNO
CXR = CXI/CXO
CTR = CTI/CTO
BBB = 1.+CTR
*
* Calculate Ternary Effective Diffusivities
*
CCC = CNO - CNI

```

```

IF (ABS(CCC).GE.(CNO/1000.)) GOTO 57
  DENN = 0.0
  GO TO 58
57  DENN = 2.*(CTR*CNR-1.)
  BBN = 1.-CNR
  DENN = DENN/(BBN*BBB)
58  CCX = CXO-CXI
  IF (ABS(CCX).GE.(CXO/1000.)) GOTO 59
  DEX = 0.0
  GOTO 61
59  DEX = 2.*(CTR*CXR-1.)
  BBX = 1.-CXR
  DEX = DEX/(BBX*BBB)
61  CONTINUE
*
* Calculate Ri's for components
*
  EPN = 2./3.
  RN = (ABS(DENN))**(EPN)
  RX = (ABS(DEX))**(EPN)
*
  RETURN
  END
*
SUBROUTINE AR (IN,TKCO,TKPO,COO,CCO,CPO,DO,DC,DP,
1             YC,YP,CCI,CPI,RC,RP,a1,e1)
*
* Subroutine to calculate anion rates for ternary exchange
*
  IMPLICIT REAL*8 (A-H,O-Z)
  INTEGER IN
*
  IF (IN.NE.1) THEN
    TKNH = 1.5D0
    TKXH = 2.4D0
    TKNX = TKNH/TKXH
  ELSE
    TKCP = TKCO/TKPO
  ENDIF
  AO = DO/DC
  AP = DP/DC
  CTO = CCO+CPO+COO
  S = (COO+CCO+CPO)*(AO*COO+CCO+AP*CPO)
*
  DENOM1 = TKCP+(1-TKCP)*YC+(TKCP-TKCO)*YP

```

```

DENOM2 = AO*TKCP+(1-AO*TKCP)*YC+(AP*TKCP-AO*TKCO)*YP
CCI = YC*(S/DENOM1/DENOM2)**0.5
IF(CCI .LE. 0.0) CCI=0.0
*   CPI = CCI*TKCP*YP/YN
CPI = ((1/a1)*YP)**(1/e1)
IF (CPI .LE. 0.0) CPI=0.0
COI = CCI*TKCO*(1-YC-YP)/YC
IF(COI .LE. 0.0) COI=0.0
CTI = CCI+COI+CPI
CCR = CCI/CCO
CPR = CPI/CPO
CTR = CTI/CTO
BBB = 1.+CTR
*
* Calculate Ternary Effective Diffusivities
*
  CCP = CPO-CPI
  IF (ABS(CCP).GE.(CPO/1000.)) GOTO 62
  DEP = 0.0
  GOTO 63
62  DEP = 2.*(CTR*CPR-1.)
  BBP = 1.-CPR
  DEP = DEP/(BBP*BBB)
63  CCC = CCO-CCI
  IF (ABS(CCC).GE.(CCO/1000.)) GOTO 64
  DEC = 0.0
  GOTO 65
64  DEC = 2.*(CTR*CCR-1.)
  BBC = 1.-CCR
  DEC = DEC/(BBC*BBB)
65  CONTINUE
*
* CALCULATE Ri's FOR SILICA and CHLORIDE
*
  EPN = 2./3.
  RP = (ABS(DEP))**(EPN)
  RC = (ABS(DEC))**(EPN)
*
  RETURN
  END
*
SUBROUTINE EQB(DISS,CNO,CXO,CCO,CPO,COO,CHO,K2,HS)
*
* Subroutine to calculate bulk phase concentrations based on silica equilibrium
*

```

```

IMPLICIT REAL*8 (A-H,O-Z)
REAL K1, K2
*
B2 = (CNO+CXO-CCO)
C2 = DISS*(1.0+K2*HS)
B3 = SQRT(B2**2.+4.*C2)
CHO = ABS(-B2+B3)/2.0
COO = DISS/CHO
*
pH = 14.+log10(COO)
*
IF (pH .LT. 9.0) THEN
*
  CPO =CPO
*
  ELSE
*
  CPO = K2*HS*COO
*
  ENDIF
*
IF( pH .GT. 11.0) THEN
*
  CPOO= 20000.*CPO*COO
*
  CPO = CPO -CPOO
*
  ELSE
*
  CPO = CPO
*
  ENDIF
  RETURN
END
*
SUBROUTINE CORRECT(YCA,YPA,YCAOLD,YPAOLD,TAU,
1      RATEC,RATEP)
*
*  subroutine to correct the bulk concentration when the
*  calculated loading exceeds unity on the resin
*
IMPLICIT REAL*8 (A-H,O-Z)
  YYY = YCA+YPA-1.0
  IF(YCA .GE. YPA) THEN
    IF(YCA .GT. 1.0) THEN
      YCA = 0.999999
      YPA = 0.0000005
      GOTO 420
    ELSE
      YPA = YPA-YYY
      IF(YPA .LE. 0.0) THEN
        YPA = 0.0000005
        YCA = 0.999999
      ENDIF
    ENDIF
  ENDIF
  IF(YPA .GT. 1.0) THEN
    YPA = 0.999999

```

```
        YCA = 0.0000005
        GOTO 420
ELSE
    YCA = YCA-YYY
    IF(YCA .LE. 0.0) THEN
        YCA = 0.0000005
        YPA =0.999999
    ENDIF
ENDIF
ENDIF
420    RATEP = (YPA-YPAOLD)/TAU
        RATEC = (YCA-YCAOLD)/TAU
RETURN
END
```

□

VITA

Sharma Pamarthy

Candidate for the Degree of

Master of Science

Thesis: DEVELOPMENT OF A COLUMN MODEL TO PREDICT
SILICA BREAKTHROUGH FOR MIXED BED ION
EXCHANGER

Major Field: Chemical Engineering

Biographical:

Personal Data: Born in Kottagudem, AP, India, November 12, 1971, the son of Lakshmi and Lakshmi Narayana Pamarthy.

Educational: Graduated from Chaithanya Kalasala Jr. College, Hyderabad, AP, India, in May 1988; received Bachelor of Technology Degree in Chemical Engineering from Osmania University in May 1992; completed requirements for the Master of Science degree with a major in Chemical Engineering at Oklahoma State University in May, 1996.

Experience: Employed as a teaching assistant, School of Chemical Engineering, Oklahoma State University, January 1993 to May 1993. Employed as a research assistant, School of Chemical Engineering, Oklahoma State University, June 1993 to August 1994. Employed as a teaching assistant, School of Chemical Engineering, Oklahoma State University, August 1994 to December 1994. Currently employed as a Manufacturing Technologist, Chemical Vapor Deposition, Applied Materials, Austin, Texas.